

Novel Interhalogen Molecules: Structures, Thermochemistry, and Electron Affinities of Dibromine Fluorides $\text{Br}_2\text{F}_n/\text{Br}_2\text{F}_n^-$ ($n = 1-6$)

Liangfa Gong, Qianshu Li,* and Wenguo Xu

Department of Chemistry, School of Science, Beijing Institute of Technology, Beijing, 100081, P R. China

Yaoming Xie and Henry F. Schaefer III*

Center for Computational Quantum Chemistry, University of Georgia, Athens, Georgia 30602-2556

Received: December 11, 2003

An investigation of the molecular structures, thermochemistry and electron affinities of the dibromine fluorides $\text{Br}_2\text{F}_n/\text{Br}_2\text{F}_n^-$ ($n = 1-6$) species has been performed employing five different hybrid Hartree–Fock/density functional theory (DFT) and pure DFT methods in conjunction with double- ζ plus polarization quality basis sets with additional s- and p-type diffuse functions, labeled as DZP++. These methods have been carefully calibrated (*Chem. Rev.* **2002**, *102*, 231) for the prediction of electron affinities. The optimized geometries and relative energies are discussed. A number of unusual structures are predicted. For example, for neutral Br_2F_3 and for the anion Br_2F_3^- , the global minimum has a divalent central fluorine atom. These structures are favored over more conventional Br–BrF₃ structures with normal Br–Br and Br–F bond distances. Similarly, for neutral Br_2F_4 , the global minimum is a F₃Br···BrF complex, favored by 14 kcal/mol over the more aesthetic D_2 symmetry F₂Br–BrF₂ structure. However, for the anion, the D_{2d} symmetry structure is the global minimum. For the Br_2F_5^- anion, a two-coordinate fluorine structure is favored over more conventional FBr–BrF₄ and F₂Br–BrF₃ structures (both ~10 kcal/mol higher) and a very reasonable looking Br–BrF₅ structure lying at ~32 kcal/mol. For neutral Br_2F_6 , a fluorine dibridged structure lies below the more “sensible” F₂Br–BrF₄ (by 32 kcal/mol) structure of C_{2v} symmetry. However, for the Br_2F_6^- anion, the F₂Br–BrF₄ structure is the global minimum. A model of sp³d and sp³d³ hybridization for the Br atomic orbitals rationalizes the fact that many bond angles in the $\text{Br}_2\text{F}_n/\text{Br}_2\text{F}_n^-$ systems are close to 90° or 180° to form T-shaped or rectangular pyramidal structures. The most reliable theoretical predictions of the adiabatic electron affinities (EA_{ad}) are 4.74 (Br₂F), 4.35 (Br₂F₂), 5.85 (Br₂F₃), 4.49 (Br₂F₄), 5.94 (Br₂F₅), and 4.20 eV (Br₂F₆). Comparisons with the analogous BrClF_n and BrF_n systems are made. The predicted dissociation energies for F removal are 26.2 (Br₂F), 46.0 (Br₂F₂), 39.6 (Br₂F₃), 44.3 (Br₂F₄), 32.9 (Br₂F₅), and 51.9 kcal/mol (Br₂F₆). The predicted dissociation energies for Br removal are 12.9 (Br₂F), 26.7 (Br₂F₂), 17.9 (Br₂F₃), 35.0 (Br₂F₄), 21.2 (Br₂F₅), and 57.1 kcal/mol (Br₂F₆). For the anions, the theoretical F atom dissociation energies are 63.2 (Br₂F⁻), 38.1 (Br₂F₂⁻), 66.6 (Br₂F₃⁻), 30.4 (Br₂F₄⁻), 57.7 (Br₂F₅⁻), and 23.8 kcal/mol (Br₂F₆⁻), and the theoretical F⁻ anion dissociation energies are 53.1 (Br₂F⁻), 65.0 (Br₂F₂⁻), 85.5 (Br₂F₃⁻), 76.3 (Br₂F₄⁻), 89.7 (Br₂F₅⁻), and 80.6 kcal/mol (Br₂F₆⁻). The predicted anion dissociation energies for removal of a Br atom are 56.6 (Br₂F⁻), 18.6 (Br₂F₂⁻), 55.6 (Br₂F₃⁻), 19.8 (Br₂F₄⁻), 56.2 (Br₂F₅⁻), and 26.5 kcal/mol (Br₂F₆⁻) and for removal of a Br⁻ anion are 38.5 (Br₂F), 44.3 (Br₂F₂⁻), 62.5 (Br₂F₃⁻), 65.6 (Br₂F₄⁻), 76.6 (Br₂F₅⁻), and 84.4 kcal/mol (Br₂F₆⁻).

Introduction

The halogens are very important nonmetallic elements with high electronegativities and strong oxidation properties. The fascinating hypervalent interhalogen compounds, such as BrF_n, BrClF_n, and Br₂F_n, are of fundamental bonding interest and of special import in atmospheric chemistry,^{1,2} due to their probable catalytic action in the depletion of the stratosphere ozone layer.^{3,4} The BrF_n and BrClF_n systems have been studied previously using theoretical methods to predict optimized structures, dissociation energies and electron affinities (EA).^{5,6} In the present work, we extend this research to the important $\text{Br}_2\text{F}_n/\text{Br}_2\text{F}_n^-$ ($n = 1-6$) series to predict the relative energies, EAs, and dissociation energies for more than 60 structures. A significant number of these structures are unique, representing bonding motifs previously unexplored.

Theoretical Methods

Five different density functional theory (DFT) or hybrid Hartree–Fock/DFT methods were used in the present research. The methods chosen have been exhaustively calibrated earlier for the prediction of atomic and molecular electron affinities. They are BHLYP (the half and half HF/DFT hybrid exchange functional⁷ combined with the Lee, Yang, and Parr correlation functional⁸), B3P86 (Becke’s three parameter functional⁹ plus Perdew’s correlation functional¹⁰), B3LYP (B3 combined with LYP), BP86 (incorporation of the Becke’s 1988 exchange functional¹¹ with P86), and BLYP (B along with LYP).

As in the earlier research,^{5,6} the standard double- ζ plus polarization basis sets augmented with diffuse functions, denoted DZP++, were used. The basis set for bromine was constructed with Ahlrichs’ standard double- ζ spd set¹² plus a set of d-type polarization functions [$\alpha_{\text{d}}(\text{Br}) = 0.389$]¹² by adding one s diffuse

* To whom correspondence should be addressed.

function [$\alpha_s(\text{Br}) = 0.0469$] and a set of p diffuse functions [$\alpha_p(\text{Br}) = 0.0465$]. The DZP++ basis set for fluorine employed in this paper was comprised of the Huzinaga–Dunning¹³ standard double- ζ set plus a set of polarization d functions [$\alpha_d(\text{F}) = 1.00$] augmented with one diffuse s [$\alpha_s(\text{F}) = 0.1049$] and a set of p [$\alpha_p(\text{F}) = 0.0826$] diffuse functions. The final contracted basis may be designated Br(15s12p6d/9s7p3d) and F(10s6p1d/5s3p1d). All the electron affinities and molecular structures have been investigated using the Gaussian 98 program suite in Beijing.¹⁴ The fine integration grid (99,590) was applied. If necessary, to show the influence of grid size, the pruned (75,302) or finer (120,974) grid was used for comparisons. The $\text{Br}_2\text{F}_n/\text{Br}_2\text{F}_n^-$ systems are sometimes sensitive to the numerical integration grid. For instance, with the (75,302) grid and the pure DFT methods, the neutral Br_2F_6 6nc is a minimum, but with the finer (99,590) grids, it has a small imaginary vibrational frequency (6i cm^{-1} with BP86 and 22i cm^{-1} with BLYP). The (120,974) grid gives a related result (2 cm^{-1} with BP86 and 22i cm^{-1} with BLYP) as the (99,590) grid. It is seen that these tiny vibrational frequencies can be very sensitive to the integration grid. Thus, the (75,302) grid, which is the default in the Gaussian program package, may not be entirely satisfactory for species containing heavy atoms such as Br, and we recommend the use of the (99,590) grid for these systems. The convergence criterion for the SCF procedure is 10^{-8} au in the density.

The geometries were optimized independently with each of the five DFT methods. The maximum force is converged to less than 10^{-5} au. The vibrational frequency analyses were carried out at each level, to get the zero point vibrational energies (ZPVE) and to assess the nature of the stationary points. We found that the ZPVE corrections for E_{Ad} are quite small, in the range 0.00–0.04 eV, except for 0.08 eV for Br_2F_6 with the BHLYP method.

Three forms of the neutral-anion energy separation are determined as differences in total energies:

The adiabatic electron affinities are determined by

$$EA_{\text{ad}} = E_{(\text{optimized neutral})} - E_{(\text{optimized anion})}$$

the vertical electron affinities by

$$EA_{\text{vert}} = E_{(\text{optimized neutral})} - E_{(\text{anion at optimized neutral geometry})}$$

and the vertical detachment energies by

$$\text{VDE} = E_{(\text{neutral at optimized anion geometry})} - E_{(\text{optimized anion})}$$

We also report the first dissociation energies for the systems studied. In general, for the types of systems considered here, BHLYP is most reliable for structural predictions, while B3LYP is best for thermochemistry.

Results and Discussions

$\text{Br}_2/\text{Br}_2^-$. Our optimized geometries and harmonic vibrational frequencies (cm^{-1}) for Br_2 are listed in Table 1. The theoretical Br–Br bond distance for the neutral ground-state Br_2 ($^1\Sigma_g^+$) ranges from 2.308 Å (BHLYP) to 2.372 Å (BLYP). The general trend of bond lengths predicted for the Br_2 is BHLYP \sim B3P86 < B3LYP < BP86 < BLYP. The DZP++ BHLYP method gives the result closest to the experimental r_e of 2.281 Å, obtained from Raman spectroscopy.¹⁵ The BHLYP method also gives the highest accuracy for the harmonic vibrational frequency, but it provides the worst dissociation energy D_e . The

TABLE 1: Bond Length (Å), Harmonic Vibrational Frequency (cm^{-1}), and Dissociation Energy in eV (kcal/mol in Parentheses) for Neutral Br_2

method	r_e	ω_e	D_e^a
BHLYP	2.308	325	1.52 (35.1)
B3P86	2.310	317	2.05 (47.3)
B3LYP	2.338	303	1.86 (42.9)
BP86	2.341	297	2.19 (50.5)
BLYP	2.372	281	1.99 (45.9)
expt	2.281 ^b	325 ^b	1.9707 (45.4) ^b

^a Total energy difference with the ZPVE correction. ^b Reference 15.

TABLE 2: Bond Length (Å), Harmonic Vibrational Frequency (cm^{-1}), and Dissociation Energy in eV (kcal/mol in Parentheses) for the Anionic Br_2^-

method	r_e	ω_e	D_e^a
BHLYP	2.927	145	1.23 (28.5)
B3P86	2.925	139	1.53 (35.4)
B3LYP	2.986	128	1.46 (33.7)
BP86	2.982	124	1.65 (38.0)
BLYP	3.058	109	1.64 (37.8)
expt	$\sim 2.6^b$	149–160 ^c	1.15 (26.5) ^d

^a Total energy difference with ZPVE corrections. ^b Reference 17. ^c Reference 18. ^d Reference 15.

best dissociation energy was predicted by BLYP, and it deviates from experiment (45.4 kcal/mol) by only 0.5 kcal/mol.

For the anionic Br_2^- ($^2\Sigma_u^+$ ground state), the reliable bond length is 2.927 Å predicted by BHLYP (Table 2). The trend for bond lengths is B3P86 \sim BHLYP < B3LYP \sim BP86 < BLYP. Since the additional electron occupies an antibonding orbital,¹⁶ the bond length is longer than that of the neutral one. Unfortunately, the experimental data^{17,18} for Br_2^- (Table 2) are not as accurate as those for the neutral Br_2 .

The present results for the $\text{Br}_2/\text{Br}_2^-$ systems are essentially the same as those obtained by the analogous DFT methods but with the pruned (75,302) grid.¹⁶ The agreement between these two grids suggests that the methods used are converged for these diatomic $\text{Br}_2/\text{Br}_2^-$ molecules.

All of $\text{Br}_2\text{F}_n/\text{Br}_2\text{F}_n^-$ structures found in this research are predicted to have Br–Br distances longer than that found experimentally (2.281 Å) for diatomic Br_2 . However, many Br–Br distances are shorter than that for Br_2^- , which displays a formal Br–Br bond order of 1/2. In the figures that follow, we depict bromine–bromine distances longer than 2.9 Å as nonbonding, i.e., atoms separated by dotted lines.

Excursus: Standard Br–F Bond Distances and Bond Energies. To draw conclusions about the nature of the novel Br_2F_n systems considered here, it is helpful to have some standards of comparison for bond distances and bond energies. Normal Br–F distances fall in the range of 1.68–1.81 Å, based upon the experimental values for BrF (1.759 Å),¹⁹ BrF₃ (1.721 and 1.810 Å),²⁰ and BrF₅ (1.680 and 1.780 Å).²¹ For the neutral radicals not yet the subjects of experimental studies, the theoretical predictions of the Br–F distances are similar, 1.83 Å (BrF₂), 1.79 (BrF₄), and 1.77 (BrF₆). The experimental Br–F distance for the BrF₄[−] anion is slightly longer (1.890 Å) based on the X-ray results for the crystal KBrF₄.²² As discussed above, the only known Br–Br bond distances are these for Br_2 (2.281 Å) and Br_2^- (~ 2.6 Å).

The only known Br–F dissociation energy is apparently that for diatomic BrF. Actually, there are two experimental dissociation energies for BrF, namely 54.9 and 58.8 kcal/mol.^{19,23} The DZP++ B3LYP prediction (58.6 kcal/mol) agrees very well with the second experiment.¹⁹ Although the other dissocia-

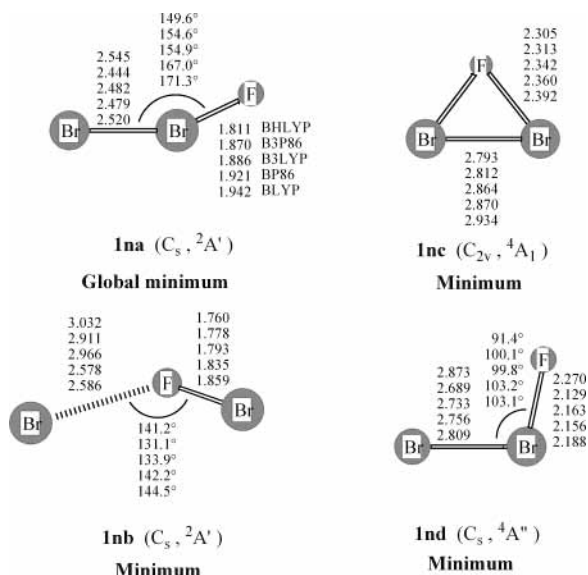


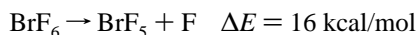
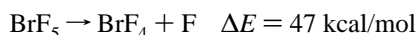
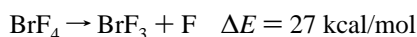
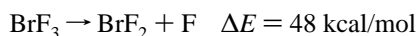
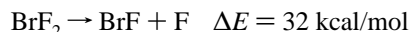
Figure 1. Optimized stationary point structures for the neutral Br_2F systems. Bond distances are in Å.

TABLE 3: Relative Energies (in eV, or in kcal/mol in Parentheses) for the Neutral Br_2F Systems^a

	BHLYP	B3P86	B3LYP	BP86	BLYP
$\text{Br} + \text{BrF}$	0.11 (2.5)	0.68 (15.7)	0.56 (12.9)	1.07 (24.6)	1.01 (23.3)
$\text{Br}_2 + \text{F}$	0.39 (9.0)	1.19 (27.5)	1.14 (26.2)	1.75 (40.3)	1.72 (39.7)
1na	0.00	0.00	0.00	0.00	0.00
1nb	0.06 (1.4)	0.65 (15.0)	0.52 (12.1)	1.01 (23.3)	0.89 (20.4)
1nc	1.44 (33.3)	1.57 (36.1)	1.44 (33.3)	1.61 (37.1)	1.48 (34.2)
1nd	1.60 (37.0)	1.75 (40.4)	1.62 (37.4)	1.64 (37.9)	1.51 (34.8)

^a Not corrected with ZPVE.

tion energies for BrF_n are not known from experiment, the theoretical values (DZP++ B3LYP)⁵ should be reliable:



For a discussion of the reliability of B3LYP thermochemistry see the recent work of Boese, Martin, and Handy.²⁴

$\text{Br}_2\text{F}/\text{Br}_2\text{F}^-$. The optimized geometries (1na–1nd) for neutral Br_2F are displayed in Figure 1, and the relative energies are listed in Table 3. The global minimum for the neutral Br_2F molecule is a slightly bent Br–Br–F structure (1na). A similar quartet state Br–Br–F structure (1nd) lies energetically above 1na by ~ 37 kcal/mol (Table 3). This quartet state has much longer Br–Br and Br–F bonds and a much smaller Br–Br–F bond angle than those of 1na (Figure 1). The other two local minima 1nb and 1nc are the F-bridged structures. Structure 1nb is a doublet state ($^2A'$) with C_s symmetry. There exists a discrepancy between the geometries predictions by the hybrid functionals and those by the pure functionals. The hybrid methods (BHLYP, B3LYP, and B3P86) predict 1nb to be a loose $\text{Br}\cdots\text{FBr}$ complex with the $\text{Br}\cdots\text{F}$ distance 2.9–3.0 Å, whereas the pure DFT methods (BP86 and BLYP) predict the longer $\text{Br}\cdots\text{F}$ distance to be ~ 2.6 Å. In either case, this $\text{Br}\cdots\text{F}$ distance is too long to be described as a Br–F single bond.

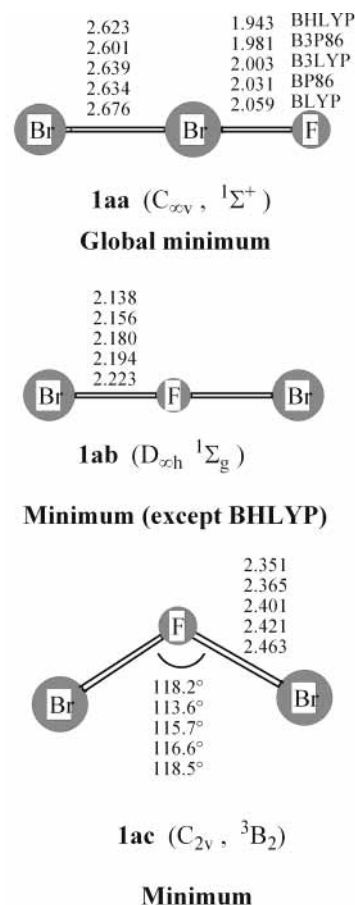


Figure 2. Optimized stationary point structures for the anionic Br_2F^- systems. Bond distances are in Å.

The shorter F–Br bond is about 1.76 Å, which is close to the F–Br bond length (1.759 Å) for isolated BrF .⁵ The energy of 1nb is higher than that of 1na by ~ 12 kcal/mol (B3LYP, Table 2). There also exists a discrepancy between the energy predictions by the hybrid functionals and those by the pure functionals. The hybrid methods predict lower relative energies (especially BHLYP, which predicts only 1.4 kcal/mol), whereas the pure density functionals predict this energy difference to be 20–23 kcal/mol. As a corollary, the BHLYP method also predicts a very low dissociation energy ($\text{Br}_2\text{F} \rightarrow \text{BrF} + \text{Br}$, Table 3). This phenomenon was also observed in the studies^{5,6,25} of ClF_n , BrF_n^- , and BrClF_n . It has been explained that the BHLYP method contains the highest fraction of Hartree–Fock theory, and H–F theory shows poor performance for bond breaking process. Another Br–F–Br structure in its quartet electronic state (4A_1) 1nc is also a local minimum. Structure 1nc is a isosceles triangle with a long Br–Br distance, and the Br–F bond (2.305 Å) in this F-bridged structure is also very long. Compared with structure 1nb, structure 1nc has a higher relative energy (~ 33 kcal/mol, Table 3).

Figure 2 shows the optimized structures for anionic Br_2F^- (1aa–1ac). Unlike the neutral Br_2F , the global minimum 1aa is a linear structure Br–Br–F ($^1\Sigma^+$ state). This is similar to the analogous anionic F–Br–F[−] and Cl–Br–F[−] systems,^{5,6} which also have linear global minima. The lowest vibrational frequency (doubly degenerate π mode) for 1aa is 160, 152, 145, 139, and 132 cm^{-1} predicted by the BHLYP, B3P86, B3LYP, BP86, and BLYP methods, respectively. The Br–Br bond distance (2.62 Å) is longer than that in the neutral structure 1na by 0.08 Å. Another linear structure with a bridging F atom is a local

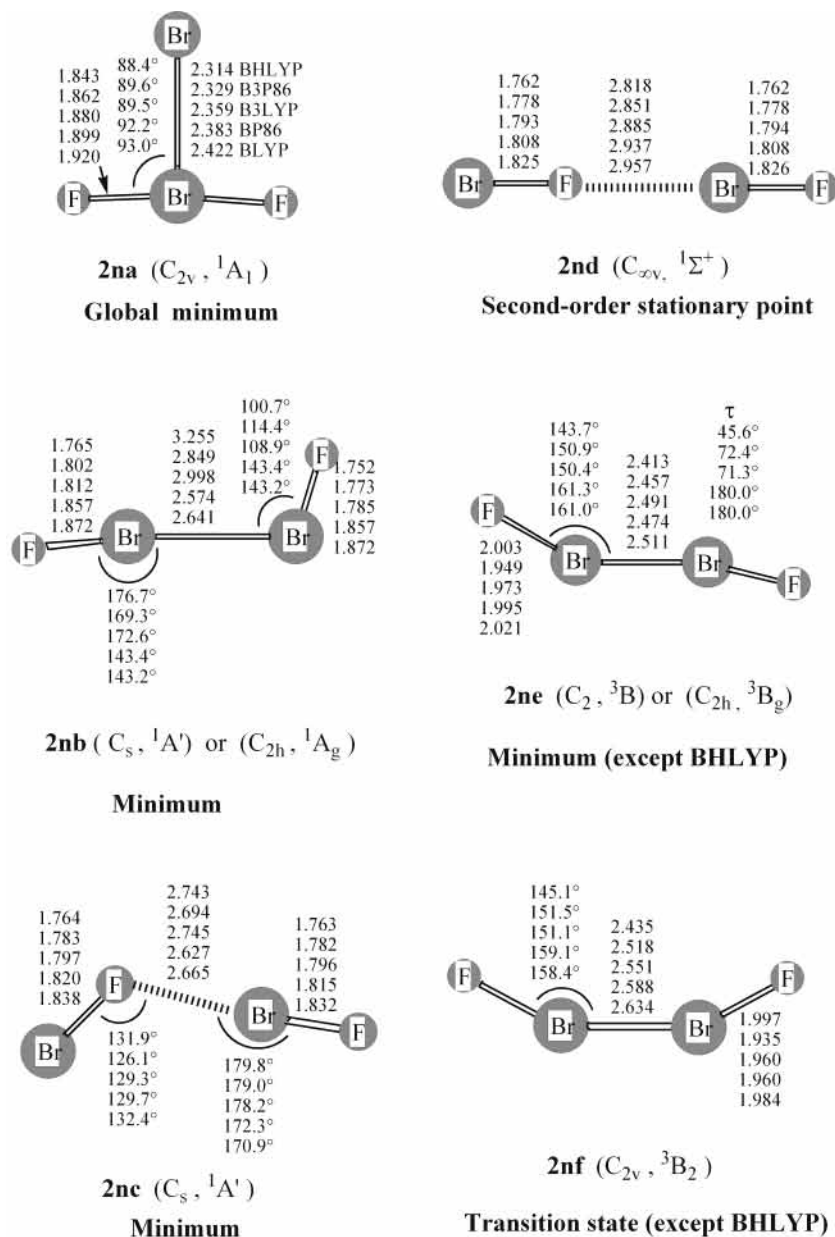


Figure 3. Optimized stationary point structures for the neutral Br_2F_2 systems. Bond distances are in Å.

TABLE 4: Relative Energies (in eV, or in kcal/mol in Parentheses) for the Anionic Br_2F^- Systems^a

	BHLYP	B3P86	B3LYP	BP86	BLYP
$\text{Br} + \text{BrF}^-$	2.20 (50.8)	2.66 (61.3)	2.45 (56.6)	2.78 (64.0)	2.63 (60.5)
$\text{Br}^- + \text{BrF}$	1.44 (33.2)	1.76 (40.6)	1.67 (38.5)	1.90 (43.8)	1.83 (42.1)
$\text{Br}_2 + \text{F}^-$	2.19 (50.5)	2.41 (55.6)	2.30 (53.1)	2.50 (57.6)	2.38 (55.0)
$\text{Br}_2^- + \text{F}$	2.12 (48.9)	2.87 (66.2)	2.74 (63.2)	3.21 (74.0)	3.11 (71.6)
1aa	0.00	0.00	0.00	0.00	0.00
1ab	1.49 (34.4)	1.21 (27.8)	1.10 (25.4)	0.95 (21.8)	0.84 (19.5)
1ac	1.51 (34.8)	1.76 (40.5)	1.59 (36.8)	1.74 (40.0)	1.57 (36.2)

^a Not corrected with ZPVE.

minimum 1ab ($1\Sigma_g^+$) except with the BHLYP method, which yields an imaginary vibrational frequency ($120i \text{ cm}^{-1}$), and leads to a $C_{\infty v}$ minimum with two unequal Br–F bonds. Structure 1ab lies above the global minimum 1aa by ~ 25 kcal/mol (B3LYP, Table 4). The triplet Br–F–Br structure 1ac is predicted to be bent (C_{2v} symmetry, 3B_2 state). It is a genuine minimum predicted with all five DFT methods and lies above 1aa by ~ 37 kcal/mol. Compared with the neutrals, the corresponding Br–F bond lengths in Br_2F^- anions are generally

longer. The order of the Br–F bond distances is BHLYP < B3P86 < B3LYP < BP86 < BLYP (Figure 2). From previous experience, the BHLYP method should give the most reliable bond distances.

$\text{Br}_2\text{F}_2/\text{Br}_2\text{F}_2^-$. For the neutral Br_2F_2 species, we investigated three types of geometric configurations, namely, the vinylidene-shaped (BrBrF_2), the acetylene-shaped (FBrBrF), and the BrFBrF structure. The optimized structures 2na–2nf are displayed in Figure 3. The first four structures (2na–2nd) lie close together energetically. The structures are in different orders energetically using the different DFT methods, but the energy difference is always less than 10 kcal/mol (Table 5). The global minimum may be the vinylidene-like C_{2v} structure in its 1A_1 state (2na), since structure 2na is predicted to have the lowest energy by three DFT (B3P86, BP86, and BLYP) methods, although it has a slightly higher energy with BHLYP and B3LYP. Prochaska et al. also suggested such a T-shaped structure for Br_2F_2 as early as 1978.²⁶ The Br–Br bond distance ranges upward from 2.31 Å (BHLYP), and the Br–F bond distance from 1.84 Å (BHLYP). These distances suggest conven-

TABLE 5: Relative Energies (in eV, or in kcal/mol in Parentheses) for the Neutral Br₂F₂ Systems^a

	BHLYP	B3P86	B3LYP	BP86	BLYP
Br + BrF ₂	0.99 (22.7)	1.34 (31.0)	1.16 (26.7)	1.37 (31.6)	1.26 (29.1)
BrF + BrF	-0.30 (-7.0)	0.17 (4.0)	0.02 (0.6)	0.43 (9.9)	0.30 (6.9)
Br ₂ F + F	1.51 (34.9)	2.15 (49.5)	2.00 (46.0)	2.33 (53.7)	2.21 (51.0)
Br ₂ + F ₂	1.27 (29.3)	1.62 (37.4)	1.56 (35.9)	1.84 (42.4)	1.81 (41.8)
2na	0.00	0.00	0.00	0.00	0.00
2nb	-0.36 (-8.3)	0.01 (0.3)	-0.08 (-1.9)	0.04 (0.8)	0.00 (0.1)
2nc	-0.42 (-9.7)	0.08 (1.8)	-0.07 (-1.7)	0.34 (7.9)	0.20 (4.7)
2nd	-0.40 (-9.3)	0.11 (2.6)	-0.05 (-1.1)	0.40 (9.1)	0.25 (5.7)
2ne	1.51 (34.7)	1.40 (33.2)	1.30 (29.9)	1.04 (23.9)	0.95 (21.9)
2nf	1.52 (35.0)	1.45 (33.5)	1.35 (31.0)	1.22 (28.2)	1.13 (26.0)

^a Not corrected with ZPVE.

tional Br–Br and Br–F single bonds. In fact, the Br–Br distance in 2na is the shortest predicted here except for the neutral diatomic Br₂.

The linear acetylene-shaped F–Br–Br–F structure is a saddle point (not shown in the Figure), whereas the trans-bent FBrBrF structure (2nb) is predicted as a genuine minimum. The pure functionals (BP86 and BLYP) predict this structure to have *C*_{2h} symmetry (¹A_g), but the hybrid functionals (BHLYP, B3LYP, and B3P86) predict a minimum with *C*_s symmetry (¹A′). These two sets (*C*_s and *C*_{2h}) of geometries are quite different. The BLYP and BP86 methods predict two equal Br–Br–F angles (143°), but the hybrid methods (BHLYP, B3LYP, and B3P86) predict two very different angles (169°–177° and 101°–114°, respectively). The hybrid methods predict the Br–Br internuclear separation to be quite long (2.8–3.3 Å), whereas BLYP and BP86 predict it to be ~2.6 Å (Figure 3). Structure 2nb has an energy very close to structure 2na, and it is either higher or lower depending on the method used. Generally, the hybrid methods predict 2nb to lie lower, whereas the pure functionals predict it higher. The B3LYP method, generally most reliable for energetics, predicts that structure 2nb is the global minimum with the energy lower than 2na by 1.9 kcal/mol. The BHLYP method places 2nb energetically even lower (8.3 kcal/mol) than 2na. The other methods predict it having the higher energy (but within 1 kcal/mol). Interestingly, the results are sensitive to the integration grid. We have tested three types of grids: (75,302), (99,590), and (120,974). With the (75,302) and (120,974) grids, the B3P86 method predicts a *C*_{2h} minimum. However, with the (99,590) grid, B3P86 yields one small imaginary frequency, which eventually collapses to a *C*_s minimum.

The singlet linear structure BrFBrF 2nd (¹Σ, *C*_{∞v}) is a second-order saddle point with all five DFT methods. It has a long Br···F distance (2.8–2.9 Å, Figure 3) and might be thought as a BrF···BrF complex. All methods predict a pair of small degenerate (<61i cm⁻¹) imaginary vibrational frequencies (π mode). Following this mode, structure 2nd collapses to a minimum structure 2nc, which has a slightly lower energy and shorter Br–Br internuclear separation. The BHLYP method predicts 2nc to have the lowest energy (lower than 2na by 9.7 kcal/mol, Table 5). The B3LYP method, usually the most reliable for thermochemistry, also predicts its energy slightly (1.7 kcal/mol) lower than 2na. However, the other DFT methods predict 2nc to have an energy higher than 2na by 7.9 (BP86), 4.7 (BLYP), and 1.8 kcal/mol (B3P86).

The triplet state structures generally have higher energies. The *C*_{2v} F–Br–Br–F structure (2nf) in its ³B₂ state is a transition state (except with BHLYP, which predicts a second-order saddle point). Following the direction of the imaginary vibrational mode (a₂ mode), we obtained structure 2ne (*C*_{2h} symmetry for the ³B_g state with the pure DFT methods, or *C*₂ symmetry for the ³B state with the hybrid methods), which is a

TABLE 6: Relative Energies (in eV, or in kcal/mol in Parentheses) for the Anionic Br₂F₂⁻ Systems^a

	BHLYP	B3P86	B3LYP	BP86	BLYP
Br + BrF ₂ ⁻	0.55 (12.7)	0.90 (20.7)	0.81 (18.6)	1.08 (25.0)	1.05 (24.2)
Br ⁻ + BrF ₂	1.92 (44.3)	1.95 (44.9)	1.92 (44.3)	1.88 (43.3)	1.88 (43.4)
BrF + BrF ⁻	1.40 (32.3)	1.68 (38.7)	1.57 (36.2)	1.81 (41.8)	1.72 (39.6)
Br ₂ F + F ⁻	2.92 (67.4)	2.89 (66.8)	2.82 (65.0)	2.76 (63.6)	2.68 (61.8)
Br ₂ F + F	1.12 (25.9)	1.67 (38.6)	1.65 (38.1)	2.00 (46.2)	2.02 (46.5)
Br ₂ + F ₂ ⁻	2.11 (48.6)	2.33 (53.6)	2.20 (50.8)	2.40 (55.3)	2.28 (52.5)
Br ₂ ⁻ + F ₂	2.61 (60.2)	2.83 (65.3)	2.82 (65.0)	2.97 (68.5)	3.00 (69.3)
2aa	0.00	0.00	0.00	0.00	0.00
2ab	0.01 (0.2)	0.17 (4.0)	0.12 (2.7)	0.19 (4.5)	0.14 (3.3)
2ac	0.04 (0.9)	0.26 (6.0)	0.20 (4.7)	0.37 (8.6)	0.32 (7.3)
2ad	0.37 (8.5)	0.34 (7.8)	0.33 (7.5)	<i>b</i>	<i>b</i>
2ae	0.46 (10.5)	0.34 (7.8)	0.34 (7.9)	0.22 (5.1)	0.23 (5.4)
2af	0.47 (10.9)	0.43 (9.9)	0.42 (9.8)	0.42 (9.7)	0.42 (9.7)
2ag	1.85 (42.6)	2.04 (46.9)	1.89 (43.5)	1.98 (45.6)	1.82 (42.0)
2ah	1.92 (44.4)	2.15 (49.6)	1.98 (45.7)	2.07 (47.8)	1.90 (43.8)

^a Not corrected with ZPVE. ^b Not a stationary point (collapse to 2ae).

minimum except for BHLYP. The BHLYP method reduces the number of imaginary frequencies for 2nf from two to one (for 2ne), so that BHLYP predicts 2ne to be a transition state. Structure 2ne has a higher energy than 2na by ~30 kcal/mol, and structure 2nf has an even higher energy (~31 kcal/mol, Table 5).

For the anionic Br₂F₂⁻ systems, we have predicted the eight structures shown in Figure 4 (2aa–2ah). The relative energies are displayed in Table 6, in which we can see that the doublet structures (2aa–2af) have energies within ~10 kcal/mol. The vinylidene-shaped BrBrF₂⁻ structure (2aa) in its ²A₁ state is the global minimum predicted by all five DFT methods. The Br–Br internuclear distance ranges from 2.95 to 3.11 Å, which is ~0.6 Å longer than that of its neutral counterpart (2na), but still in the range of that found^{17,18} in the laboratory for Br₂⁻. The linear BrFBrF structure 2ac (*C*_{∞v}, ²Σ) is a second-order saddle point with a pair of degenerate vibrational frequencies (e.g., 82i cm⁻¹ with B3LYP). It lies energetically above 2aa by ~5 kcal/mol (Table 6). Following the normal mode associated with the imaginary vibrational frequencies, 2ac collapses to the bent structure 2ab (*C*_s, ²A′), which lies above 2aa by ~3 kcal/mol. There are three Br–F bonds in 2ab, but these three bond distances are all distinct (Figure 4). Another linear structure FBrBrF 2af (*D*_{∞h}, ²Σ_g⁺) is a second-order saddle point with degenerate (π mode) vibrational frequencies. The Br–Br bond distance is shorter than that of Br₂⁻ by ~0.2 Å, and the Br–F bond distance is shorter than that of BrF⁻ by ~0.3 Å. Related along the potential surface, the trans-bent FBrBrF structure 2ae (*C*_{2h}, ²A_g) is either a minimum (predicted by BP86 and BLYP) or a transition state with a tiny imaginary frequency (55i, 24i, and 30i cm⁻¹ predicted by BHLYP, B3P86, and B3LYP, respectively). This means that 2ae is either a minimum or nearly identical energetically to a nearby minimum. Following the normal mode related to the imaginary frequency, the hybrid DFT methods predict a minimum 2ad with *C*_s symmetry in its ²A′ electronic state.

The quartet states 2ag (*C*_s, ⁴A′) and 2ah (*C*_s, ⁴A′) have significantly higher energies than the doublet ground state (> 40 kcal/mol, Table 6). The cis structure for the ⁴A′ state (2ah) is a transition state with a small imaginary vibrational frequency (34i–41i cm⁻¹, related to the torsion mode). Following this torsion mode leads to a genuine minimum (2ag), which is a trans structure with *C*_s symmetry. The trans structure lies energetically above 2aa by ~44 kcal/mol, whereas the cis structure 2ah lies above 2aa by ~46 kcal/mol.

Br₂F₃/Br₂F₃⁻. Our optimized geometries for neutral Br₂F₃ (3na–3nf) are displayed in Figure 5. For the neutral radicals,

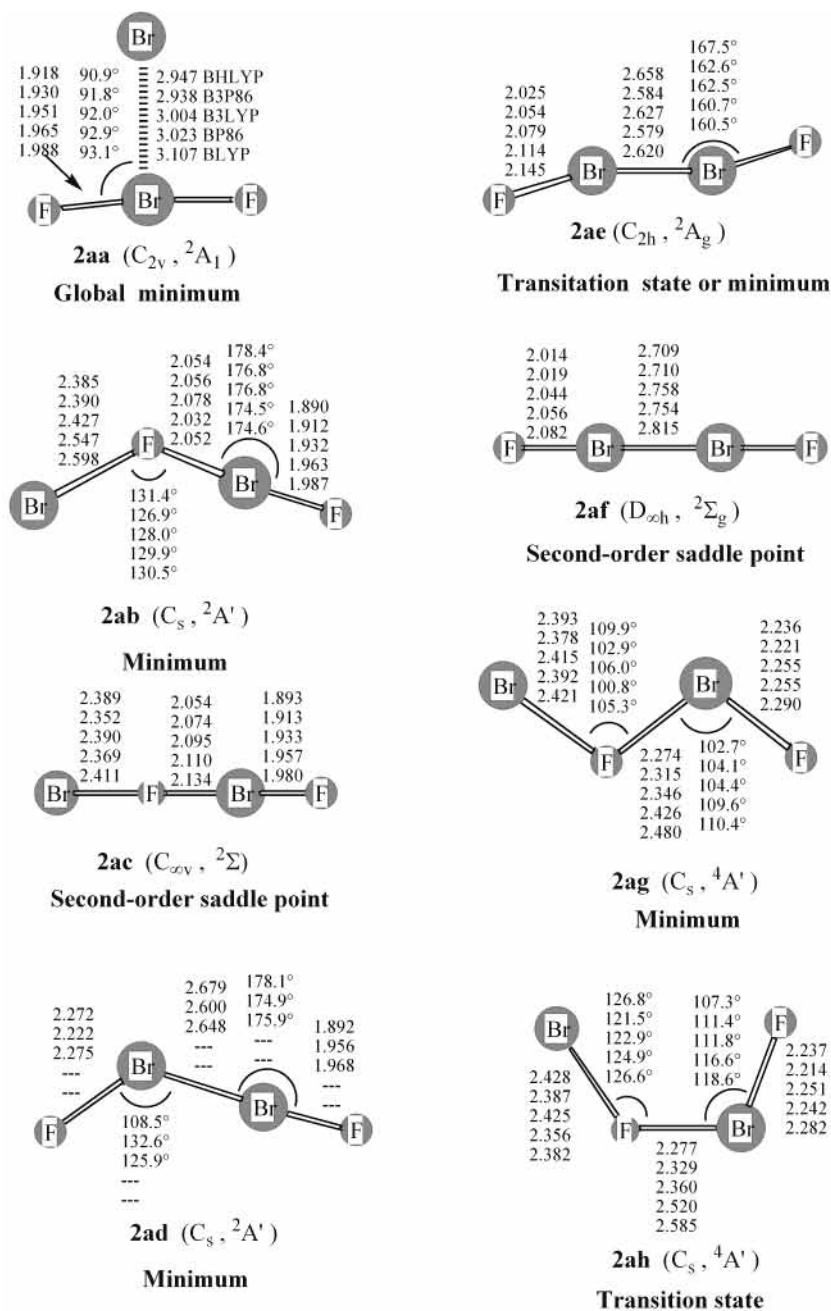


Figure 4. Optimized stationary point structures for the anionic Br_2F_2^- systems. Bond distances are in Å.

the chain $\text{F}-\text{Br}-\text{F}-\text{Br}-\text{F}$ structure **3na** ($C_{2v}, {}^2B_2$) is the global minimum except for the BHLYP method, which predicts **3na** to lie slightly (0.5 kcal/mol) above **3nd**. The two terminal $\text{Br}-\text{F}$ bond distances are predicted to be 1.78 Å, corresponding to normal single bonds. The two middle $\text{Br}-\text{F}$ bond distances are ~ 2.10 Å, too long to be called single bonds, but too short to be described as the molecular complex $\text{FBr}\cdots\text{F}\cdots\text{BrF}$. Structure **3na** is particularly interesting because it appears to be an example of an unprecedented divalent fluorine compound. The $\text{Br}-\text{F}-\text{Br}$ angle is close to a right angle ($\sim 87^\circ$), and the two $\text{F}-\text{Br}-\text{F}$ angles are almost linear ($\sim 176^\circ$).

There is also a structure similar to **3na** in its excited 2B_1 state (not shown in Figure 5) with a slightly higher energy (by < 5 kcal/mol). A stationary point with $\text{F}-\text{Br}-\text{BrF}_2$ configuration (**3nb**) has also C_{2v} symmetry (2B_1 state). It is a genuine minimum predicted by the BP86 and BLYP methods, but a transition state by the hybrid B3P86 and B3LYP methods (with a small imaginary vibrational frequency $\sim 30i$ cm^{-1}), and a third-order

stationary point by the BHLYP method. These three hybrid methods predict a C_s minimum (**3nb**) in its ${}^2A'$ state. The $\text{Br}-\text{Br}$ bond distance in **3nb** is predicted to be 2.62–2.69 Å, except by BHLYP, which predicts a much longer (3.69 Å) $\text{Br}-\text{Br}$ separation. Structure **3nb** lies above the global minimum **3na** by ~ 7 kcal/mol (Table 7). For the carbyne-like structure $\text{Br}-\text{BrF}_3$ (**3nc**), the BHLYP method predicts a C_{2v} (2B_1 state) minimum with a long (3.5 Å) $\text{Br}-\text{Br}$ distance, while the other methods predict a C_s minimum with a shorter (2.5–2.6 Å) $\text{Br}-\text{Br}$ bond (Figure 5). Structure **3nc** lies above the global minimum **3na** by 15 kcal/mol.

Another possible Br_2F_3 structure may be designated $\text{Br}-\text{F}-\text{BrF}_2$. At first we optimized the structure within the constraint of C_{2v} symmetry, and obtained a stationary point **3nf**. The BHLYP method predicts **3nf** to be a transition state with an imaginary vibrational frequency ($24i$ cm^{-1}) related to the b_2 mode, whereas the other four methods predict a second-order stationary point with two imaginary vibrational frequencies

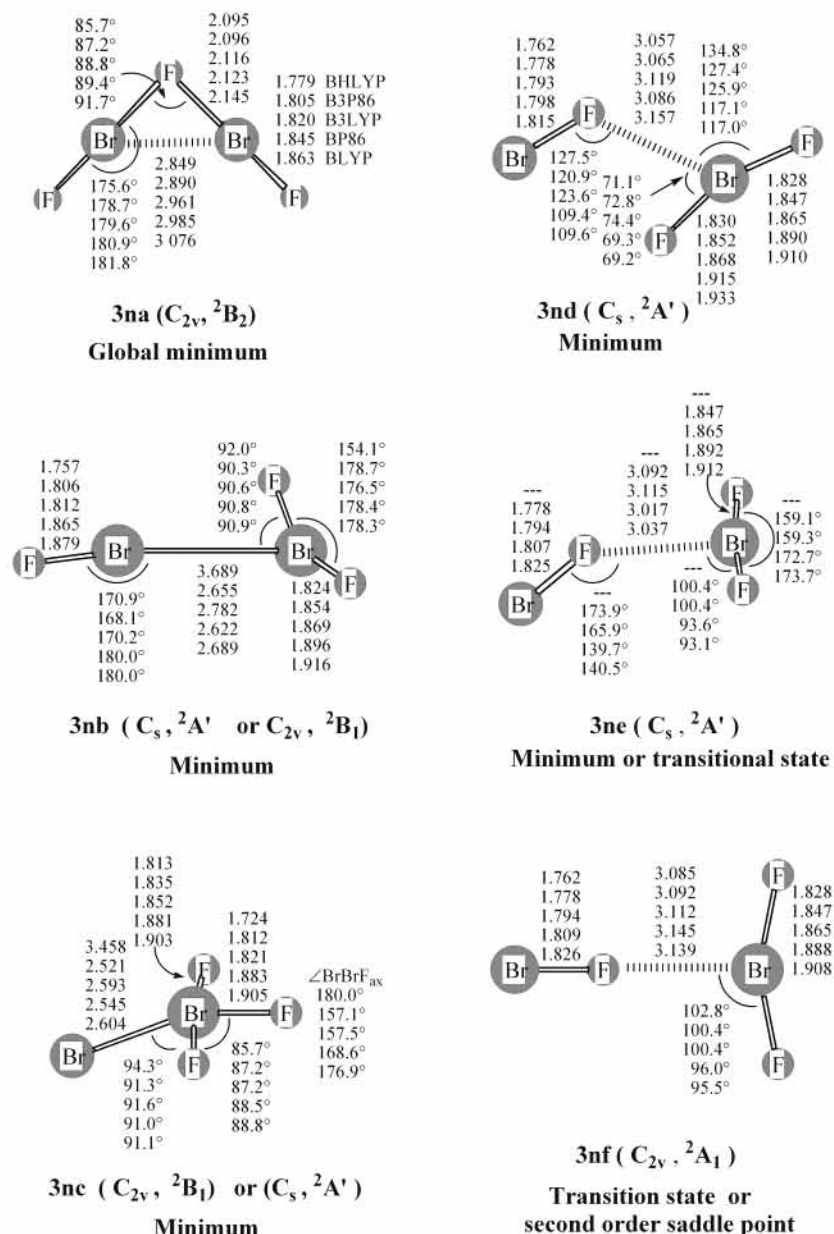


Figure 5. Optimized stationary point structures for the neutral Br_2F_3 systems. Bond distances are in Å.

TABLE 7: Relative Energies (in eV, or in kcal/mol in parentheses) for the Neutral Br_2F_3 System^a

	BHLYP	B3P86	B3LYP	BP86	BLYP
$\text{Br} + \text{BrF}_3$	0.32 (7.3)	0.80 (18.5)	0.78 (17.9)	1.13 (26.0)	1.17 (27.0)
$\text{BrF} + \text{BrF}_2$	0.06 (1.3)	0.42 (9.7)	0.34 (7.9)	0.60 (13.9)	0.54 (12.4)
$\text{Br}_2\text{F}_2 + \text{F}$	1.00 (23.0)	1.73 (40.0)	1.72 (39.6)	2.20 (50.7)	2.20 (50.7)
$\text{Br}_2\text{F} + \text{F}_2$	1.88 (43.4)	2.17 (49.9)	2.14 (49.4)	2.29 (52.8)	2.29 (52.8)
3na	0.00	0.00	0.00	0.00	0.00
3nb	0.07 (1.7)	0.31 (7.1)	0.31 (7.2)	0.17 (3.8)	0.20 (4.5)
3nc	0.24 (5.7)	0.56 (13.0)	0.64 (14.8)	0.46 (10.6)	0.53 (12.2)
3nd	-0.02 (-0.5)	0.37 (8.6)	0.29 (6.7)	0.54 (12.4)	0.46 (10.6)
3ne	<i>b</i>	0.38 (8.7)	0.29 (6.7)	0.57 (13.2)	0.49 (11.3)
3nf	-0.01(-0.3)	0.38 (8.7)	0.29 (6.7)	0.58 (13.4)	0.50 (11.6)

^a Not corrected with ZPVE. ^b Same as 3nf.

related to the b_2 ($25i-47i$ cm^{-1}) and b_1 ($9i-54i$ cm^{-1}) modes. Following the b_2 mode, there exists a genuine minimum 3nd, which has C_s symmetry (${}^2A'$ state) with all five atoms in a plane. This structure may be considered as a $\text{BrF}\cdots\text{BrF}_2$ complex, since the Br-F distance separating the two parts is more than ~ 3 Å. The BHLYP method predicts 3nd lying even lower than 3na

by 0.5 kcal/mol (Table 7), but the (usually) energetically superior B3LYP method predicts 3nd to lie higher than the global minimum 3na by ~ 7 kcal/mol. Following the b_1 mode of 3nf, one locates a genuine minimum 3ne with the B3P86 and B3LYP methods, also with C_s symmetry (${}^2A'$ state) but having two F atoms out of the reflection plane. With the pure DFT methods, 3ne is a transition state with a small imaginary vibrational frequency which leads to 3nd. Structure 3ne also has a long $\text{BrF}\cdots\text{BrF}_2$ distance (> 3 Å), and it might also be considered as a complex. Structure 3ne has almost the same energy as that of 3nf (Table 7). We have investigated several quartet structures, but those stationary points have rather high energies, so they are not reported in this paper.

The anionic Br_2F_3^- (3aa-3ad) are shown in Figure 6. We obtained a chain-shaped global minimum $\text{F}-\text{Br}-\text{F}-\text{Br}-\text{F}^-$ with C_{2v} symmetry in its 1A_1 ground state (3aa). Compared with its neutral counterpart 3na, the anionic structure has longer internuclear separations and a larger Br-F-Br bond angle. However, 3aa shares with 3na the unusual feature of an apparently divalent fluorine atom. The $\text{F}-\text{Br}-\text{BrF}_2^-$ minimum

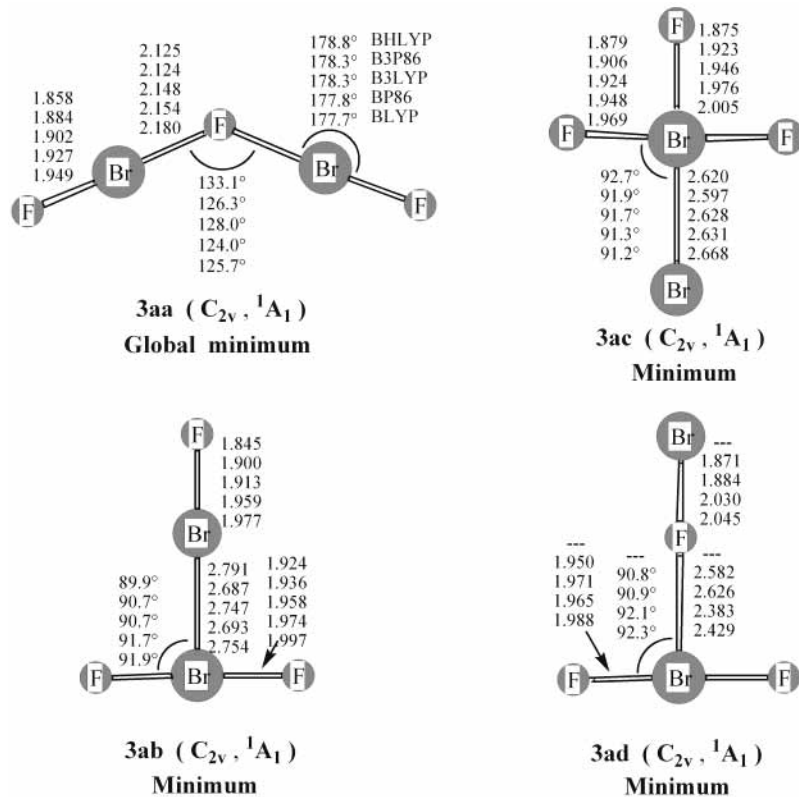


Figure 6. Optimized stationary point structures for the anionic Br_2F_3^- systems. Bond distances are in Å.

TABLE 8: Relative Energies (in eV, or in kcal/mol in Parentheses) for the Anionic Br_2F_3^- System^a

	BHLYP	B3P86	B3LYP	BP86	BLYP
Br + BrF_3^-	2.40 (55.1)	2.54 (58.5)	2.42 (55.6)	2.50 (57.5)	2.42 (55.9)
$\text{Br}^- + \text{BrF}_3$	2.77 (62.6)	2.63 (60.7)	2.71 (62.5)	2.57 (59.1)	2.68 (61.6)
$\text{BrF} + \text{BrF}_2^-$	1.13 (26.0)	1.21 (27.7)	1.16 (26.8)	1.15 (28.6)	1.21 (27.8)
$\text{BrF}^- + \text{BrF}_2$	3.27 (75.3)	3.15 (62.6)	3.06 (70.2)	2.92 (67.3)	2.78 (64.1)
$\text{Br}_2\text{F}_2 + \text{F}^-$	2.50 (57.7)	2.96 (68.3)	2.89 (66.6)	3.13 (72.1)	3.08 (71.0)
$\text{Br}_2\text{F}_2 + \text{F}^-$	3.91 (90.2)	3.71 (85.5)	3.71 (85.5)	3.56 (82.0)	3.55 (81.8)
$\text{Br}_2\text{F} + \text{F}_2^-$	4.22 (97.4)	4.09 (94.4)	3.95 (91.2)	3.78 (87.1)	3.64 (83.9)
$\text{Br}_2\text{F}^- + \text{F}_2$	2.99 (69.0)	2.92 (67.3)	2.97 (68.4)	2.89 (66.7)	2.98 (68.7)
3aa	0.00	0.00	0.00	0.00	0.00
3ab	0.41 (9.4)	0.21 (4.8)	0.27 (6.2)	0.11 (2.4)	0.17 (3.8)
3ac	1.08 (25.0)	0.61 (14.0)	0.71 (16.3)	0.37 (8.5)	0.47 (10.8)
3ad	<i>b</i>	1.16 (26.8)	1.13 (26.0)	0.86 (19.8)	0.82 (19.1)

^a Not corrected with ZPVE. ^b Dissociated to $\text{BrF} + \text{BrF}_2^-$.

(3ab) is a T-shaped structure (C_{2v} symmetry, 1A_1 state), and it lies above the global minimum 3aa by about 6 kcal/mol. The bond distances of structure 3ab are mostly longer than those of its neutral counterpart 3nb. The carbyne-like $\text{Br}-\text{BrF}_3^-$ structure 3ac also has C_{2v} symmetry, and it is higher than 3aa by ~16 kcal/mol. Still another C_{2v} minimum $\text{Br}-\text{F}-\text{BrF}_2^-$ (3ad) lies energetically above 3aa by 19–27 kcal/mol predicted by four DFT methods, whereas the BHLYP method predicts an untenable structure, which dissociates into $\text{BrF} + \text{BrF}_2^-$.

$\text{Br}_2\text{F}_4/\text{Br}_2\text{F}_4^-$. The global minimum of the neutral Br_2F_4 is a peculiar planar $\text{FBr}-\text{BrF}_3$ structure with C_s symmetry (4na in Figure 7) predicted by four DFT methods except for BHLYP, which presents an imaginary vibrational frequency ($17i \text{ cm}^{-1}$). Following the corresponding normal mode, a minimum with C_1 symmetry 4nb is predicted by BHLYP with slightly (0.3 kcal/mol) lower energy (Table 9). In 4nb, five atoms ($\text{F}-\text{Br}-\text{F}-\text{Br}-\text{F}$) are nearly in a plane and another F atom almost perpendicular to the plane by a $\text{Br}-\text{F}_x$ bond (Figure 7). The other four DFT methods also predict 4nb to be a genuine minimum, but having a slightly (~0.2 kcal/mol) higher energy

TABLE 9: Relative Energies (in eV, or in kcal/mol in Parentheses) for the Neutral Br_2F_4 System^a

	BHLYP	B3P86	B3LYP	BP86	BLYP
Br + BrF_4	1.67 (38.9)	0.92 (21.0)	1.52 (35.0)	1.48 (34.1)	1.47 (33.9)
$\text{BrF} + \text{BrF}_3$	0.17 (3.8)	0.21 (4.7)	0.17 (3.9)	0.38 (8.7)	0.32 (7.4)
$\text{BrF}_2 + \text{BrF}_2$	1.20 (27.5)	0.99 (22.8)	0.87 (20.0)	0.79 (18.3)	0.65 (14.9)
$\text{Br}_2\text{F}_3 + \text{F}$	1.78 (41.0)	2.06 (47.4)	1.92 (44.3)	2.22 (51.1)	2.07 (47.8)
$\text{Br}_2\text{F}_2 + \text{F}_2$	2.14 (49.4)	2.08 (47.9)	2.06 (47.6)	2.17 (50.2)	2.15 (49.6)
$\text{BrF} + \text{BrF} + \text{F}_2$	1.84 (42.4)	2.25 (51.9)	2.09 (48.2)	2.60 (60.1)	2.45 (56.5)
4na	0.00	0.00	0.00	0.00	0.00
4nb	-0.01(-0.3)	0.04 (1.0)	0.01 (0.2)	0.23 (5.2)	0.17 (3.9)
4nc	0.02 (0.5)	0.10 (2.3)	0.05 (1.1)	0.29 (6.7)	0.21 (4.9)
4nd	1.06 (24.5)	0.55 (12.6)	0.61 (14.1)	0.26 (6.1)	0.24 (5.6)
4ne	2.00 (46.0)	0.96 (22.0)	0.87 (20.1)	0.35 (8.1)	0.24 (5.6)
4nf	1.27 (29.2)	0.76 (17.5)	0.90 (20.7)	0.64 (14.8)	0.74 (17.1)
4ng	2.57 (59.2)	1.96 (45.2)	2.01 (46.3)	1.72 (39.8)	1.74 (40.2)

^a Not corrected with ZPVE.

than 4na (Table 9). The planar BrFBrF_3 structure 4nc (C_s , $^1A'$) is another low-lying minimum with relative energy ~1 kcal/mol above 4na. Structures 4na–c can be reasonably taken as $\text{F}_2\text{BrF}\cdots\text{BrF}$ or $\text{F}_3\text{Br}\cdots\text{FBr}$ complexes due to the long (2.3–2.8 Å) $\text{Br}\cdots\text{F}$ distances. The structure F_2BrBrF_2 (4nd) is predicted to be either a D_{2h} minimum (planar) by the pure functionals (BP86 and BLYP) or a D_2 minimum (twisted with a dihedral angle of 65°) by the hybrid methods (BHLYP, B3P86, and B3LYP). The energy for the D_{2h} structure 4nd is only ~6 kcal/mol above 4na as predicted by the pure DFT methods, but it is quite large (14 kcal/mol, B3LYP) for the D_2 structure with the hybrid methods (Table 9). However, structure 4nd is more conventional in that all bond distances represent normal single bonds. This point is repeated elsewhere in these theoretical studies: unconventional structures are sometimes preferred energetically to these with traditional single bond distances.

A planar doubly F-bridging structure $\text{FBr}(\mu-\text{F})_2\text{BrF}$ (4ne) with C_{2h} symmetry is predicted to be a minimum with low

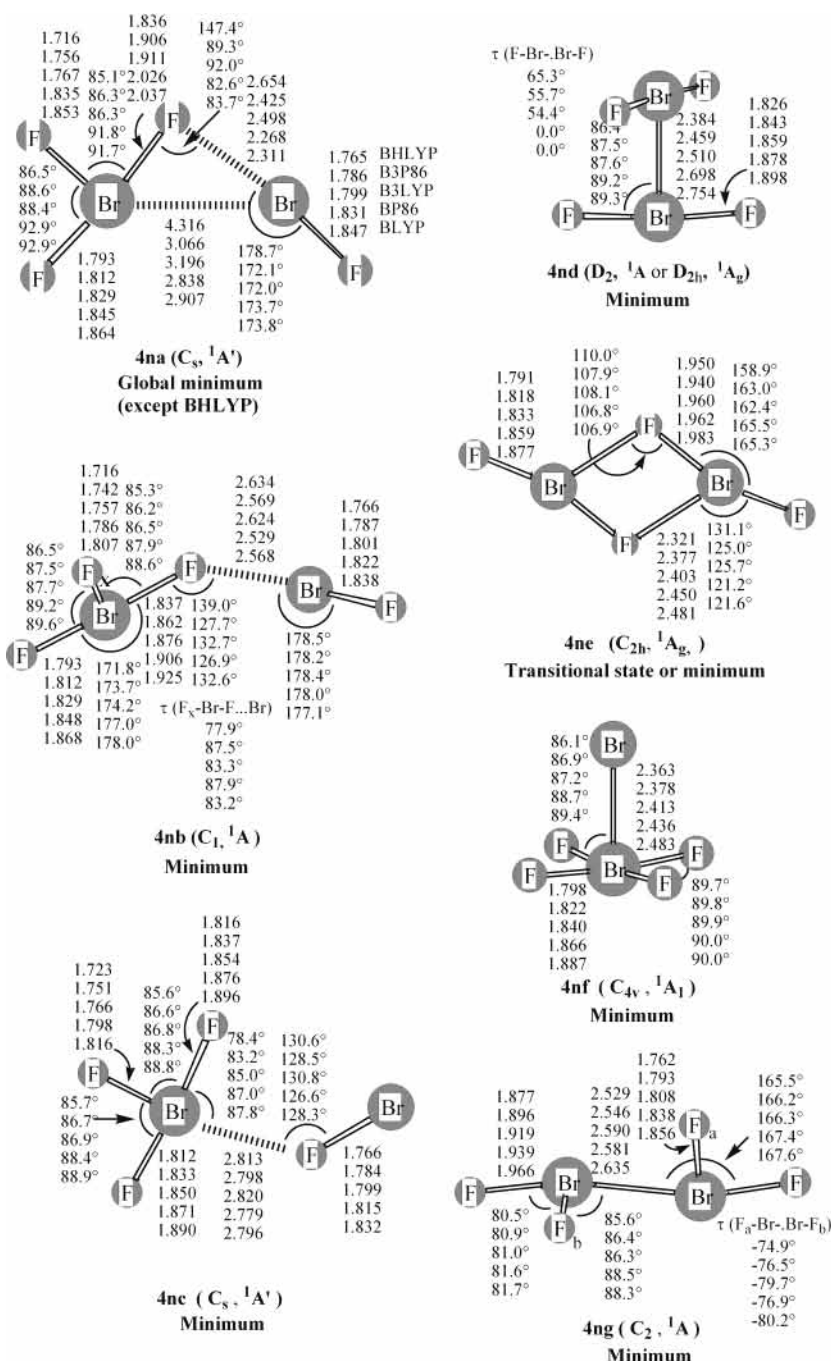


Figure 7. Optimized stationary point structures for the neutral Br_2F_4 systems. Bond distances are in Å.

relative energy (6–8 kcal/mol) by the pure DFT methods but to be a transition state with higher energy (20 kcal/mol, B3LYP) by the hybrid methods (Table 9). The normal mode (b_u) of the imaginary frequency (243i, 74i, and 72i cm^{-1} for BHLYP, B3P86, and B3LYP) leads to the global minimum 4na. The square pyramidal $BrBrF_4$ structure 4nf (C_{4v} symmetry, 1A_1 state), analogous in some respects to BrF_5 , is a minimum with energy higher than 4na by ~21 kcal/mol. Another $F_2Br-BrF_2$ structure 4ng with C_2 symmetry (1A) and all bond distances normal is also a minimum. Four atoms (F–Br–Br–F) line up, with the other two F atoms nearly perpendicular to this axis with F_aBrBrF_b dihedral angle 75° . Structure 4ng has much higher energy (~46 kcal/mol) above 4na, and it is not thermodynamically stable due to its relative energy being ~26 kcal/mol higher than that of 2 BrF_2 (Table 9). We also tried to optimize the F_3BrBrF arrangement, but it collapses to 4na.

For the anionic $Br_2F_4^-$, unlike the neutrals, the global minimum is the staggered D_{2d} $F_2BrBrF_2^-$ structure in its 2B_2 state (4aa, Figure 8). It could be regarded as a $F_2Br\cdots BrF_2$ system with bond order one-half, since the Br–Br distance is ~0.6 Å longer than the neutral counterpart 4nd, and the last electron occupies the Br–Br antibonding orbital (b_2). A closely related planar structure with D_{2h} symmetry is a transition state (not shown) with energy higher than the D_{2d} structure by 2 kcal/mol (B3LYP). The anionic structure similar to the C_{2h} neutral 4ne is a low-lying structure 4ab. Structure 4ab is predicted to be a C_{2h} minimum by BP86 and BLYP, but a C_s minimum by B3P86 and B3LYP. It lies above the global minimum 4aa by only 0.9 (BLYP), 1.4 (BP86), 2.3 (B3LYP), and 3.2 (B3P86) kcal/mol (Table 10). The BHLYP method predicts the C_s structure to be a transition state with very low energy (lower than 4aa by 0.4 kcal/mol), and the imaginary vibrational

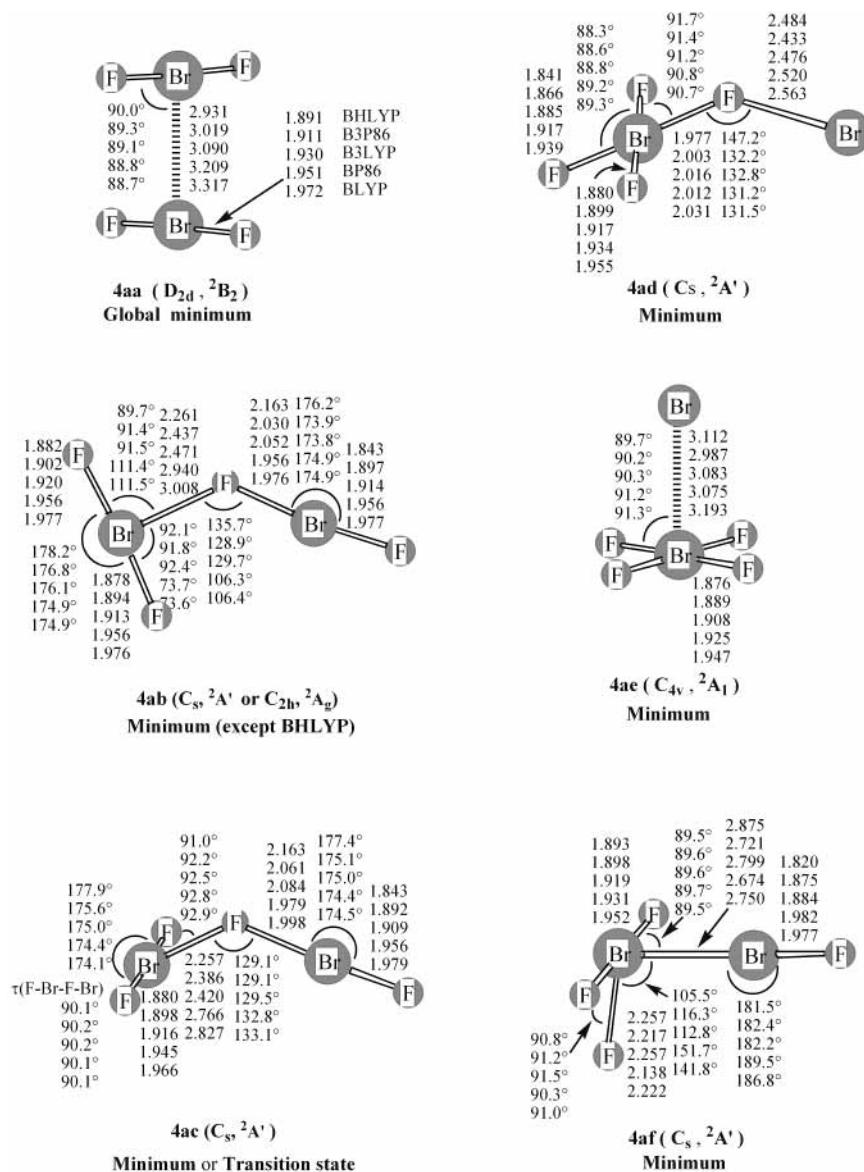


Figure 8. Optimized stationary point structures for the anionic $Br_2F_4^-$ systems. Bond distances are in Å.

TABLE 10: Relative Energies (in eV, or in kcal/mol in Parentheses) for the Anionic $Br_2F_4^-$ System^a

	BHLYP	B3P86	B3LYP	BP86	BLYP
Br + BrF_4^-	0.59 (13.6)	0.91 (21.0)	0.86 (19.8)	1.13 (26.1)	1.15 (26.7)
Br^- + BrF_4	2.76 (63.7)	2.75 (63.6)	2.85 (65.6)	2.71 (62.6)	2.85 (65.7)
BrF + BrF_3^-	0.87 (20.2)	1.30 (30.0)	1.20 (27.6)	1.53 (35.5)	1.45 (33.5)
BrF^- + BrF_3	2.01 (46.3)	2.29 (53.0)	2.28 (52.6)	2.48 (57.3)	2.50 (57.6)
BrF_2 + BrF_2^-	0.90 (20.7)	1.13 (26.1)	1.08 (24.9)	1.23 (28.4)	1.19 (27.5)
Br_2F_3 + F^-	3.32 (76.7)	3.39 (78.2)	3.31 (76.3)	3.36 (77.6)	3.30 (76.1)
$Br_2F_3^-$ + F	0.41 (9.5)	1.42 (32.7)	1.32 (30.4)	2.01 (46.3)	1.95 (45.0)
Br_2F_2 + F_2^-	3.12 (71.9)	3.36 (77.6)	3.28 (75.6)	3.46 (79.7)	3.38 (77.9)
$Br_2F_2^-$ + F_2	2.28 (52.6)	2.66 (61.4)	2.63 (60.7)	2.90 (66.8)	2.91 (67.2)
4aa	0.00	0.00	0.00	0.00	0.00
4ab	-0.02 (-0.4)	0.14 (3.2)	0.10 (2.3)	0.06 (1.4)	0.04 (0.9)
4ac	-0.03 (-0.7)	0.14 (3.2)	0.10 (2.3)	0.09 (2.1)	0.06 (1.4)
4ad	0.25 (5.8)	0.44 (10.2)	0.43 (9.9)	0.54 (12.4)	0.54 (12.5)
4ae	0.42 (9.7)	0.47 (10.9)	0.51 (11.7)	0.50 (11.6)	0.56 (12.9)
4af	0.36 (8.3)	0.58 (13.4)	0.57 (13.3)	0.64 (14.9)	0.69 (15.8)

^a Not corrected with ZPVE.

frequency leads it to another C_s structure (4ac) with insignificantly lower energy (Table 10). Structure 4ac is predicted to be the global minimum only by BHLYP, and it is a local minimum with almost the same energy (within 0.01 kcal/mol) as 4ab predicted by B3P86 and B3LYP. However, 4ac is a

transition state (above 4aa by 1–2 kcal/mol) according to the BP86 and BLYP methods. Following the corresponding normal mode, the BP86 and BLYP methods take 4ac back to the C_{2h} minimum 4ab. In summary, structures 4aa, 4ab, and 4ac are nearly energetically degenerate, representing a very flat region

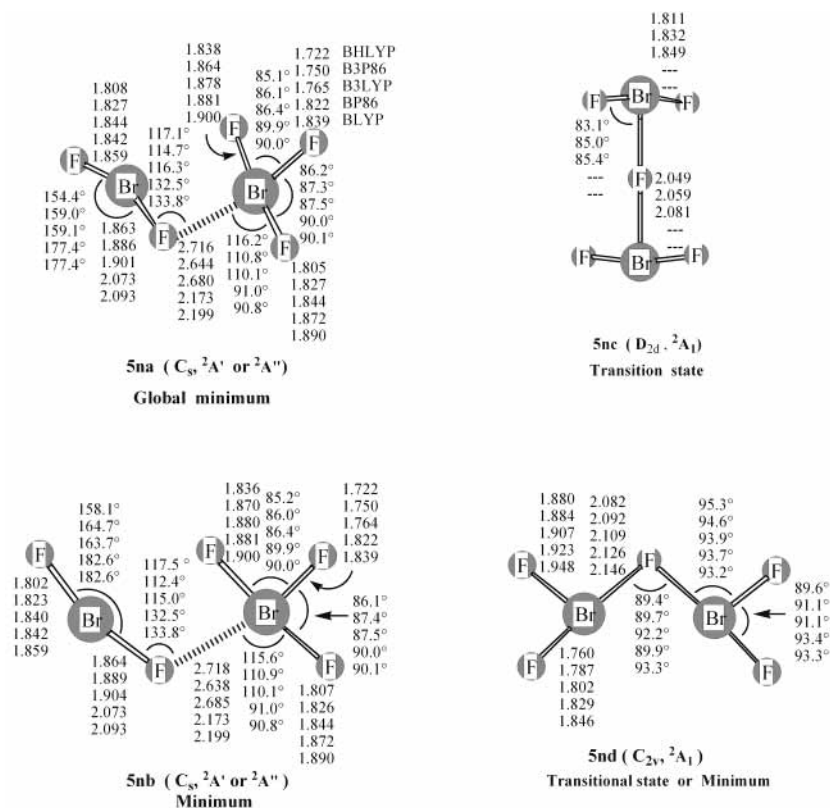


Figure 9. Optimized stationary point structures for the neutral Br_2F_5 systems. Bond distances are in Å.

of the potential energy hypersurface. The BHLYP method predicts 4ac to be the global minimum, but other methods (usually more reliable for energetic predictions) conclude that the energetic sink is 4aa. BHLYP predicts 4ab to be a transition state collapsing to 4ac, but the BP86 and BLYP methods predict 4ac to be a transition state collapsing to 4ab, whereas the B3LYP and B3P86 methods predict both to be local minima with virtually the same energy. Structure 4ad F_3BrFBr^- (C_s symmetry, ${}^2A'$) is another local minimum, lying above 4aa by ~ 10 kcal/mol (Table 10). Its geometry may be described as $\text{F}_3\text{BrF}^- \cdots \text{Br}$, which is different from the corresponding neutral structure 4nc, the latter described as $\text{F}_3\text{Br} \cdots \text{FBr}$. The pentavalent C_{4v} (2A_1) BrBrF_4^- structure 4ae is also a local minimum, in which the Br–Br bond (~ 3 Å) is much longer than that for the neutral counterpart 4nf. The energy of 4ae is ~ 12 kcal/mol higher than that of 4aa. The nonplanar $\text{F}_3\text{Br} \cdots \text{BrF}$ structure 4af with C_s symmetry (${}^2A'$) lies above 4aa by ~ 13 kcal/mol.

$\text{Br}_2\text{F}_3/\text{Br}_2\text{F}_5^-$. Our optimized geometries for the neutral Br_2F_5 structures (5na–5nd) are displayed in Figure 9. Structures of the general form $\text{F}_2\text{Br} \cdots \text{BrF}_3$ were considered but found to fall apart to $\text{F}_2\text{Br} + \text{BrF}_3$. The energetically lowest structure 5na with C_s symmetry is in its ${}^2A'$ state using the BHLYP, B3P86, and B3LYP methods, but is a ${}^2A''$ state with the BP86 and BLYP methods. The lowest vibrational frequency is very small ($< 50 \text{ cm}^{-1}$). It seems that structure 5na is a loose complex best designated $\text{FBrF} \cdots \text{BrF}_3$. The pure DFT methods predict the $\text{F} \cdots \text{Br}$ distance (for the ${}^2A''$ state) to be 2.17 Å (BP86) and 2.20 Å (BLYP), whereas the hybrid methods predict it (for the ${}^2A'$ state) much longer: ~ 2.7 Å. The bond angles predicted for ${}^2A''$ state are also different from those predicted for ${}^2A'$ state. Like 5na, the structure 5nb is predicted to have a ${}^2A'$ ground state with the hybrid methods, and a ${}^2A''$ ground state with the pure DFT methods. The ${}^2A'$ state has an almost identical geometry to 5na except for a different F–Br–F angle in the F–Br–F fragment, and it has an energy very close to 5na (within < 0.3

kcal/mol), whereas the ${}^2A''$ state predicted by the BP86 and BLYP methods is in fact identical to 5na (Figure 9). Thus, we cannot be certain whether 5na or 5nb is the global minimum. The hybrid methods predict a D_{2d} transition state 5nc ($\text{F}_2\text{Br} \cdots \text{F} \cdots \text{BrF}_2$), but the pure DFT methods failed to locate it. The energy of 5nc is higher than that of 5na by ~ 18 kcal/mol. The normal mode (b_2) related to the 5nc imaginary vibrational frequency leads to structure 5na. A high-lying (~ 26 kcal/mol above 5na) structure 5nd with C_{2v} symmetry (in its 2A_1 state) is predicted to be a genuine minimum by the pure DFT methods but to be a transition state by the hybrid methods. The imaginary vibrational frequency from the hybrid methods directs 5nd to 5na.

The anionic Br_2F_5^- system has more stable structures (5aa–5af, seen in Figure 10) than the neutrals. The relative energies of these systems are listed in Table 12. The global minimum 5aa has C_s symmetry with a FBrFBrF_3 structure (Figure 10). A major difference in geometry between 5aa and 5na is that the former is not planar. We tried to optimize a constrained planar structure (similar to 5na), but it is a transition state and collapses eventually to 5aa. Structure 5aa is a F-bridged structure with the two comparable F–Br bond distances (2.20 and 2.07 Å with BHLYP), which are much shorter than the $\text{F} \cdots \text{Br}$ bond in neutral 5na, suggesting a stronger Br–F connection than its neutral counterpart. Thus, it would not be correct to call 5aa a molecular complex. The second low-lying structure 5ab has C_{4v} symmetry, lying above 5aa by ~ 10 kcal/mol. Structure 5ab might be regarded as a $\text{FBr} \cdots \text{BrF}_4^-$ complex due to the long Br–Br bond (~ 3 Å). However, it should be noted that this Br–Br distance is no longer than that for the bond of formal order one-half in diatomic Br_2^- except BHLYP. The C_{2v} $\text{F}_3\text{Br} \cdots \text{BrF}_2$ structure 5ac is a local minimum lying above 5aa by ~ 10 kcal/mol. The D_{2d} structure 5ad, unlike its neutral counterpart 5nc, is also a genuine minimum except with the BHLYP method. Structure 5ad lies above 5aa (by 23 kcal/mol, B3LYP) with all DFT

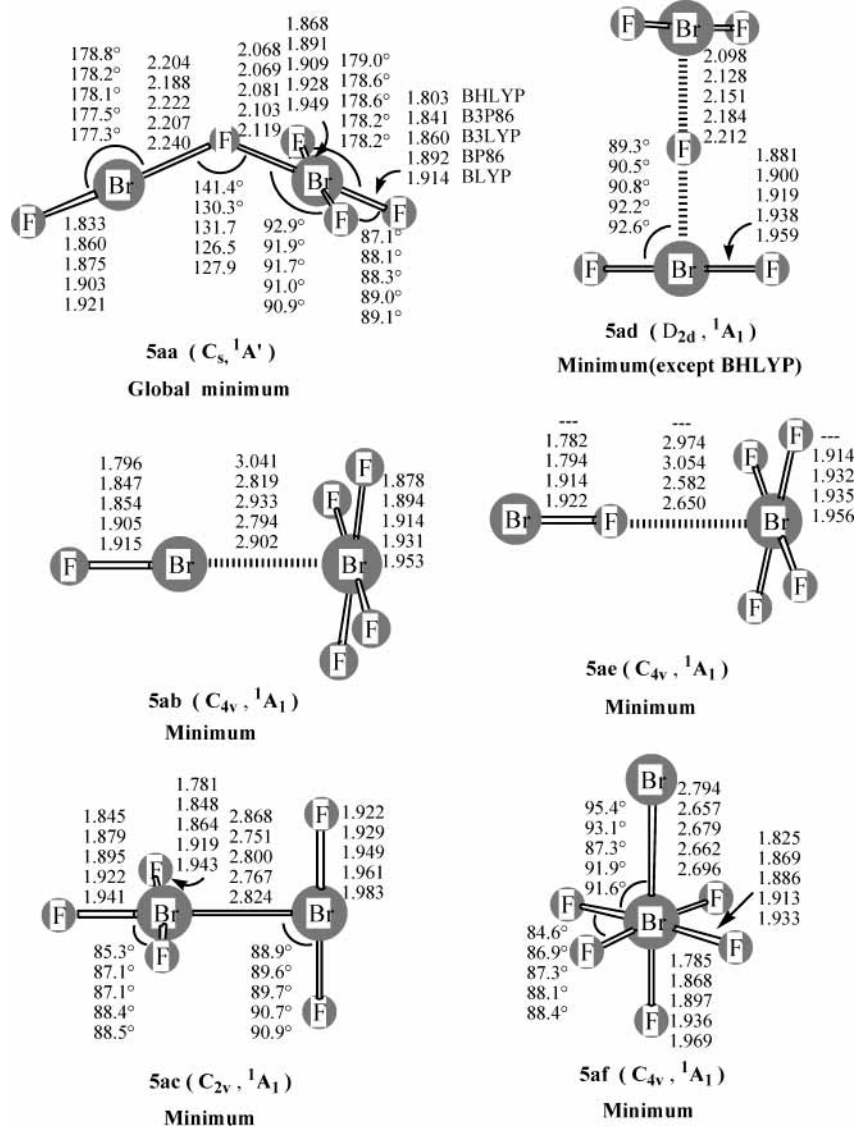


Figure 10. Optimized stationary point structures for the anionic $Br_2F_5^-$ systems. Bond distances are in Å.

TABLE 11: Relative Energies in eV (or in kcal mol⁻¹ in Parentheses) for the $Br_2F_5^-$ System^a

	BLYP	B3P86	B3LYP	BP86	BLYP
Br + BrF ₅	0.70 (16.3)	0.78 (18.1)	0.92 (21.2)	1.17 (27.0)	1.31 (30.2)
BrF + BrF ₄	0.47 (11.0)	0.38 (8.8)	0.41 (9.4)	0.54 (12.5)	0.57 (13.0)
BrF ₂ + BrF ₃	0.25 (5.6)	0.19 (4.4)	0.20 (4.5)	0.38 (8.8)	0.38 (8.7)
Br ₂ F ₄ + F	0.71 (16.4)	1.47 (34.0)	1.43 (32.9)	2.02 (46.7)	2.02 (46.6)
Br ₂ F ₃ + F ₂	1.85 (42.8)	1.82 (41.9)	1.77 (40.9)	2.00 (46.1)	1.98 (45.6)
5na	0.00	0.00	0.00	0.00	0.00
5nb	0.01 (0.3)	0.00 (0.1)	0.01 (0.12)	0.17 (3.8)	0.17 (3.9)
5nc	1.18 (27.3)	0.79 (18.2)	0.78 (18.0)		
5nd	1.54 (35.6)	1.09 (25.1)	1.12 (25.8)	1.05 (24.1)	1.08 (24.9)

^a Not corrected with ZPVE.

methods, which predicts 5ad a transition state with very high energy (37 kcal/mol above 5aa). Again, we conclude that the BHLYP energetics are in error. The BrF···BrF₄⁻ structure 5ae with C_{4v} symmetry is a local minimum of even higher energy (except with the BHLYP method, which predicts it to dissociate into BrF + BrF₄⁻). The Br—BrF₅ structure 5af is a hypervalent structure, (perhaps reminiscent of the valence isoelectronic XeF₆), lying above 5aa by ~33 kcal/mol.

Br₂F₆/Br₂F₆⁻. Our optimized geometries for neutral Br₂F₆ are shown in Figure 11. The global minimum 6na has a doubly F-bridged structure with C_{2h} symmetry in its 1A_g state. With

TABLE 12: Relative Energies in eV (or in kcal mol⁻¹ in Parentheses) for the $Br_2F_5^-$ System^a

	BHLYP	B3P86	B3LYP	BP86	BLYP
Br + BrF ₅ ⁻	2.40 (55.3)	2.53 (58.3)	2.44 (56.2)	2.47 (57.0)	2.44 (56.2)
Br ⁻ + BrF ₅	3.23 (74.4)	3.12 (71.9)	3.32 (76.6)	3.12 (71.9)	3.36 (77.6)
BrF + BrF ₄ ⁻	0.82 (19.0)	0.87 (20.1)	0.83 (19.1)	0.91 (21.0)	0.87 (20.0)
BrF ⁻ + BrF ₄	3.76 (86.8)	3.62 (83.4)	3.60 (83.0)	3.37 (77.7)	3.36 (77.5)
BrF ₂ + BrF ₃ ⁻	2.40 (55.2)	2.43 (56.0)	2.30 (53.0)	2.26 (52.0)	2.13 (49.1)
BrF ₂ ⁻ + BrF ₃	1.39 (32.1)	1.47 (34.0)	1.48 (34.2)	1.53 (35.3)	1.54 (35.6)
Br ₂ F ₄ + F ⁻	3.71 (85.5)	3.95 (91.1)	3.89 (89.7)	3.89 (89.8)	3.87 (89.2)
Br ₂ F ₄ ⁻ + F	2.16 (49.8)	2.61 (60.3)	2.50 (57.7)	2.75 (63.3)	2.64 (60.8)
Br ₂ F ₃ + F ₂ ⁻	4.28 (98.7)	4.25 (97.9)	4.06 (93.6)	4.00 (92.3)	3.82 (88.0)
Br ₂ F ₃ ⁻ + F ₂	1.94 (44.7)	2.32 (53.4)	2.25 (51.8)	2.51 (57.9)	2.47 (57.0)
5aa	0.00	0.00	0.00	0.00	0.00
5ab	0.48 (11.2)	0.38 (8.7)	0.42 (9.7)	0.31 (7.2)	0.37 (8.6)
5ac	0.55 (12.7)	0.36 (8.3)	0.42 (9.6)	0.24 (5.6)	0.29 (6.7)
5ad	1.59 (36.7)	1.02 (23.4)	0.99 (22.9)	0.62 (14.2)	0.57 (13.2)
5ae	— ^b	0.95 (21.9)	0.91 (21.0)	0.83 (19.2)	0.81 (18.6)
5af	1.92 (44.2)	1.27 (29.2)	1.41 (32.5)	0.90 (20.7)	1.04 (24.1)

^a Not corrected with ZPVE. ^b Dissociates to BrF + BrF₄⁻.

the pure density functional methods (BP86 and BLYP) 6na actually has D_{2h} symmetry, and is reminiscent of diborane. When the D_{2h} symmetry is constrained, structure 6nb is identical to 6na with the BP86 and BLYP methods, but 6nb is a transition state with the hybrid methods (BHLYP, B3P86, and B3LYP).

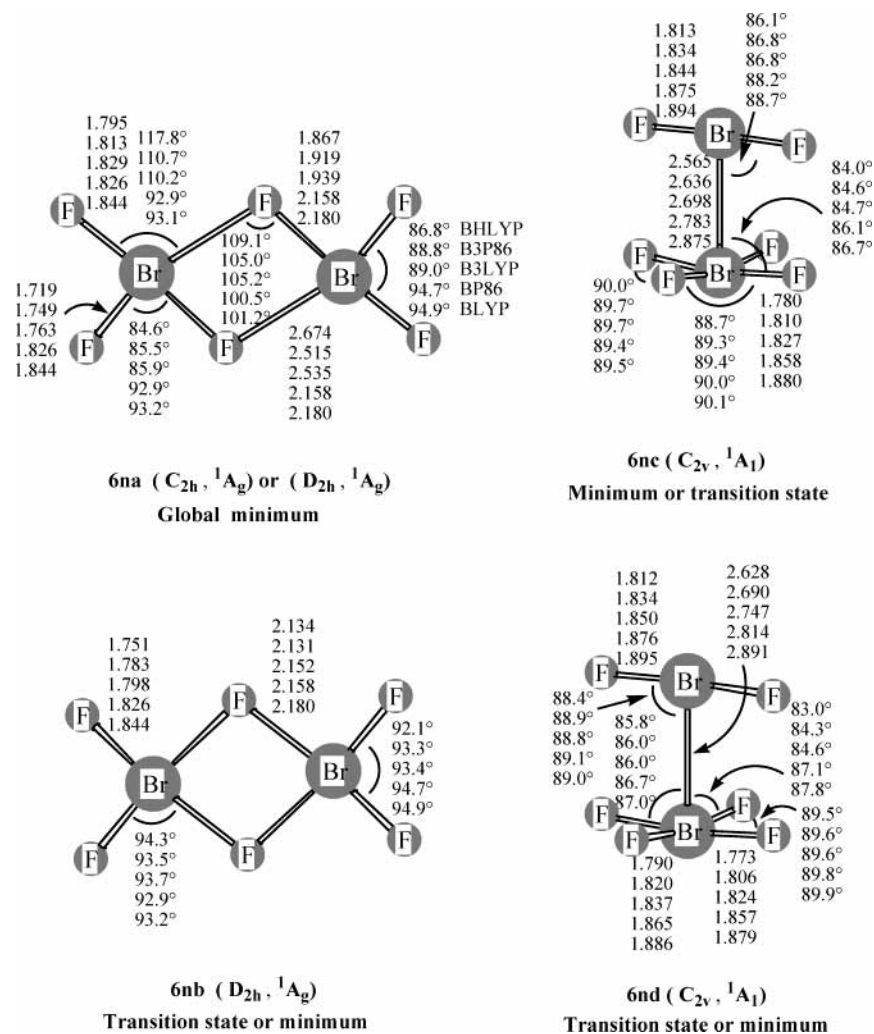


Figure 11. Optimized stationary point structures for the neutral Br_2F_6 systems. Bond distances are in Å.

TABLE 13: Relative Energies in eV (or in kcal mol⁻¹ in Parentheses) for the Br_2F_6 System^a

	BHLYP	B3P86	B3LYP	BP86	BLYP
Br + BrF ₆	2.52 (58.0)	2.40 (55.3)	2.47 (57.1)	2.52 (58.1)	2.69 (62.1)
BrF + BrF ₅	0.57 (13.2)	0.55 (12.8)	0.64 (14.7)	0.75 (17.2)	0.84 (19.4)
BrF ₂ + BrF ₄	1.63 (37.5)	1.32 (30.4)	1.26 (29.1)	1.06 (24.4)	1.00 (23.1)
BrF ₃ + BrF ₃	0.37 (8.5)	0.34 (7.9)	0.35 (8.0)	0.48 (11.0)	0.49 (11.2)
Br ₂ F ₅ + F	1.79 (41.3)	2.42 (55.9)	2.25 (51.9)	2.54 (58.6)	2.40 (55.3)
Br ₂ F ₄ + F ₂	1.87 (43.1)	2.18 (50.3)	2.10 (48.5)	2.33 (53.6)	2.30 (53.1)
6na	0.00	0.00	0.00	0.00	0.00
6nb	0.35 (8.0)	0.07 (1.7)	0.06 (1.5)	0.00	0.00
6nc	2.03 (46.9)	1.28 (29.6)	1.39 (32.2)	0.89 (20.4)	0.95 (21.9)
6nd	2.21 (51.0)	1.37 (31.5)	1.45 (33.4)	0.88 (20.3)	0.93 (21.4)

^a Not corrected with ZPVE.

The energy of 6nb is only slightly (<2 kcal/mol) higher than that of 6na with the B3LYP and B3P86 methods, whereas it is 8 kcal/mol higher with the less reliable BHLYP method (Table 13). We also found two high-lying F_2BrBrF_4 structures 6nc and 6nd. Both structures display C_{2v} symmetry (Figure 11) and appear to incorporate genuine Br–Br bonds. This is another example where the structure with “normal” single bonds lies energetically above the unconventional structure. The hybrid methods (BHLYP, B3P86, and B3LYP) methods predict the staggered structure 6nc to be a genuine minimum, and predict that the eclipsed structure 6nd is a transition state. In contrast, the pure DFT methods (BP86 and BLYP) predict structure 6nd to be the minimum but 6nc a transition state. Note that the small imaginary torsional vibrational frequency is sensitive to the

integration grid. With the sparse grid (75,302), the BP86 and BLYP predict all real vibrational frequencies for structure 6nc, but with the finer grids (99,590) or (120,974), the BLYP method predicts one small imaginary frequency. Structures 6nc and 6nd lie energetically above 6na by ~33 kcal/mol (Table 13).

For the $Br_2F_6^-$ anion, the optimized structures are shown in Figure 12. The global minimum 6aa is a C_{2v} $F_2Br\cdots BrF_4^-$ complex (2A_1 state) with a large Br–Br internuclear separation 3.18 (B3P86) ~ 3.69 Å (BLYP). However, the BHLYP method predicts two small imaginary vibrational frequencies $b_2, 29i; b_1, 15i$ cm⁻¹. Following the normal modes related to the imaginary frequencies, the BHLYP geometry optimization leads to the F-bridged structure 6ab (C_s symmetry at the $^2A'$ state), which is the global minimum predicted by the BHLYP method, with energy lower than 6aa by 8 kcal/mol (Table 14). With the other hybrid methods (B3P86 and the more reliable B3LYP), structure 6ab is also a minimum, but lies above 6aa by ~2 kcal/mol. The pure DFT methods (BP86 and BLYP) predict structure 6ab to possess a tiny imaginary frequency (<5i cm⁻¹), and the energy higher than the 6aa by 9–10 kcal/mol (Table 14). A planar structure 6ac, which has similar geometry and energy to 6ab, is predicted to be a transition state. The corresponding normal mode leads 6ac back to structure 6ab. A fascinating D_{2d} $F_3Br-BrF_3$ structure 6ad with normal Br–Br and Br–F bond distances is found to be a minimum (except BHLYP) lying above 6aa by ~12 kcal/mol. The BHLYP method predicts an imaginary vibrational frequency, which leads back to structure

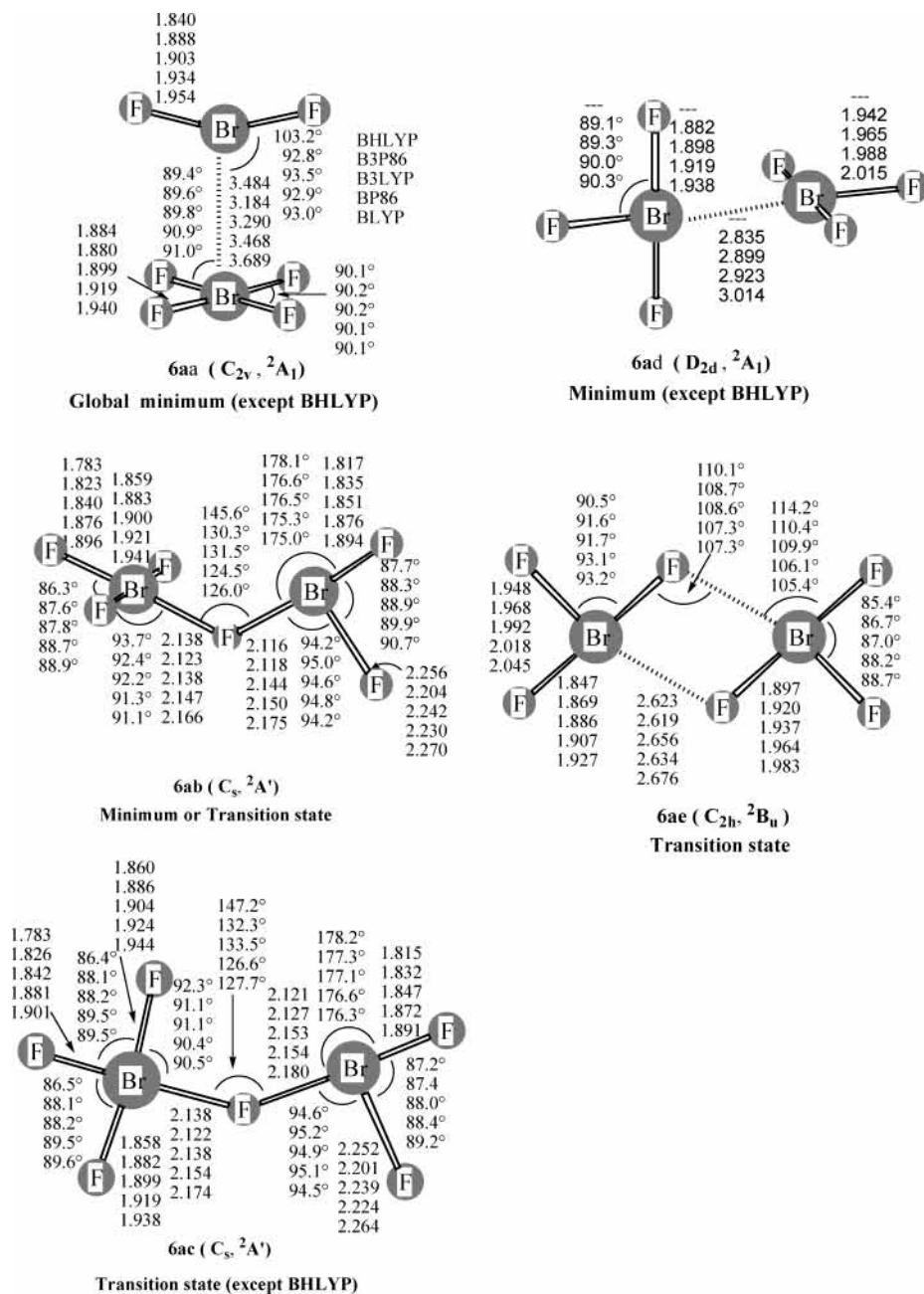


Figure 12. Optimized stationary point structures for the anionic $Br_2F_6^-$ systems. Bond distances are in Å.

TABLE 14: Relative Energies in eV (or in kcal mol⁻¹ in Parentheses) for the $Br_2F_6^-$ System^a

	BHLYP	B3P86	B3LYP	BP86	BLYP
Br + BrF ₆ ⁻	1.14 (26.2)	1.17 (26.9)	1.15 (26.5)	1.30 (30.0)	1.37 (31.7)
Br ⁻ + BrF ₆	3.30 (76.2)	3.43 (79.0)	3.66 (84.4)	3.75 (86.4)	4.05 (93.4)
BrF ₂ ⁻ + BrF ₄	1.04 (24.0)	1.31 (30.3)	1.33 (30.7)	1.49 (34.4)	1.53 (35.2)
BrF ₂ + BrF ₄ ⁻	0.24 (5.5)	0.52 (11.9)	0.46 (10.6)	0.70 (16.2)	0.66 (15.3)
BrF ₃ ⁻ + BrF ₃	0.78 (18.1)	1.29 (29.7)	1.23 (28.4)	1.64 (37.7)	1.60 (36.8)
Br ₂ F ₅ + F ⁻	3.05 (70.4)	3.61 (83.2)	3.50 (80.6)	3.69 (85.1)	3.60 (83.1)
Br ₂ F ₅ ⁻ + F	0.06 (1.3)	1.13 (26.1)	1.03 (23.8)	1.82 (42.0)	1.76 (40.5)
Br ₂ F ₄ + F ₂ ⁻	2.56 (59.0)	3.32 (76.6)	3.17 (73.1)	3.61 (83.2)	3.50 (80.8)
Br ₂ F ₄ ⁻ + F ₂	1.58 (36.5)	2.03 (46.9)	1.96 (45.2)	2.33 (53.6)	2.28 (52.5)
6aa	0.00	0.00	0.00	0.00	0.00
6ab	-0.35 (-8.0)	0.14 (3.1)	0.08 (1.8)	0.45 (10.4)	0.41 (9.4)
6ac	-0.34 (-7.8)	0.15 (3.4)	0.08 (1.9)	0.47 (10.7)	0.42 (9.7)
6ad	0.43 (9.8)	0.48 (11.0)	0.50 (11.6)	0.60 (13.8)	0.63 (14.5)
6ae	0.81 (18.6)	0.73 (16.9)	0.69 (15.9)	0.72 (16.7)	0.69 (15.9)

^a Not corrected with ZPVE.

6ab. The doubly F-bridged structure 6ae with C_{2h} symmetry, analogous to the neutral global minimum 6aa, is a transition

state with all five DFT methods, and, structure 6ae lies above the global minimum 6aa by ~16 kcal/mol.

Electron Affinities of the $Br_2F_n/Br_2F_n^-$ Systems. The reliability of DFT methods in the prediction of the electron affinities for the F, Cl, and Br atoms was tested by Pak et al.⁵ and Ignatyev et al.⁶ It was shown that the smallest overall mean error was produced by BLYP for the EA of these atoms.⁶ A comprehensive review about the theoretical prediction of electron affinities with DFT methods was reported in 2002 by Rienstra-Kiracofe et al.²⁷ and the average absolute deviation for 91 molecules is only 0.14 eV with the DZP++ B3LYP or DZP++ BLYP methods and 0.18 eV with the BP86 method.

Our predicted three types of neutral-anion energy separations for the $Br_2F_n/Br_2F_n^-$ ($n = 1-6$) systems are listed in Table 15. Generally speaking, the B3P86 method predicts much higher EA_{ad}, whereas the other four methods predict EAs in reasonable agreement with each other. To confirm the reliability of these methods, the EAs for the Br₂ molecule, for which the experi-

TABLE 15: Adiabatic Electron Affinities (EA_{ad}) and Vertical Electron Affinities (EA_{vert}) for the Neutral Br₂ and Br_nF_n (*n* = 1–6) Systems and Vertical Detachment Energies (VDE) for the Anionic Br₂[−] and Br₂F_n[−] (*n* = 1–6) Systems in eV (or in kcal/mol in Parentheses)

			BHLYP	B3P86	B3LYP	BP86	BLYP
Br ₂	1Σ _g ⁺ ← 2Σ _u ⁺	EA _{ad}	3.01 (69.4)	3.57 (81.8)	3.11 (71.6)	3.06 (70.5)	2.95 (68.1)
		EA _{vert}	1.68 (38.8)	2.33 (53.8)	1.90 (43.8)	1.94 (44.7)	1.84 (42.5)
		VDE	4.35 (100.2)	4.77 (110.0)	4.31 (99.4)	4.18 (96.4)	4.06 (93.7)
Br ₂ F	1na ← 1aa	EA _{ad}	4.74 (109.4)	5.23 (120.5)	4.71 (108.6)	4.52 (104.2)	4.34 (100.1)
		EA _{vert}	4.00 (92.2)	4.62 (106.5)	4.14 (95.5)	4.25 (98.1)	4.14 (95.4)
		VDE	5.01 (115.5)	5.49 (126.5)	4.94 (113.9)	4.66 (107.5)	4.48 (103.4)
Br ₂ F ₂	2na ← 2aa	EA _{ad}	4.35 (100.3)	4.75 (109.6)	4.37 (100.7)	4.37 (100.7)	4.14 (95.6)
		EA _{vert}	2.96 (68.2)	3.56 (82.1)	3.19 (73.5)	3.19 (73.5)	3.17 (73.1)
		VDE	5.72 (131.9)	5.83 (134.4)	5.41 (124.7)	5.04 (116.3)	8.93 (205.1)
Br ₂ F ₃	3na ← 3aa	EA _{ad}	5.85 (135.0)	5.98 (137.9)	5.53 (127.6)	5.12 (118.1)	5.03 (115.9)
		EA _{vert}	5.89 (135.7)	5.95 (137.2)	5.44 (125.4)	5.01 (115.6)	4.87 (112.2)
		VDE	14.14 (326.1)	13.96 (321.9)	13.45 (310.2)	13.01 (300.0)	12.86 (296.4)
Br ₂ F ₄	4na ← 4aa	EA _{ad}	4.49 (103.5)	5.34 (123.2)	4.93 (113.8)	4.91 (113.3)	4.90 (113.1)
		EA _{vert}	2.34 (53.9)	3.11 (71.8)	2.74 (63.2)	2.93 (67.6)	2.97 (68.4)
		VDE	6.62 (152.7)	6.66 (153.5)	6.26 (144.3)	5.74 (132.5)	5.68 (131.0)
Br ₂ F ₅	5na ← 5aa	EA _{ad}	5.94 (136.9)	6.48 (149.5)	6.01 (138.6)	5.63 (129.9)	5.52 (127.3)
		EA _{vert}	4.41 (101.7)	5.32 (122.7)	4.86 (112.0)	5.41 (124.7)	5.29 (121.9)
		VDE	7.01 (161.6)	8.16 (188.1)	7.80 (179.9)	7.39 (170.5)	5.85 (134.8)
Br ₂ F ₆	6na ← 6aa	EA _{ad}	4.20 (96.8) ^a	5.19 (119.7)	4.79 (110.4)	4.91 (113.2)	4.88 (112.5)
		EA _{vert}	2.30 (53.1)	3.44 (79.4)	3.08 (71.0)	3.05 (70.4)	3.08 (71.0)
		VDE	7.97 (183.7)	7.28 (167.8)	6.91 (163.2)	10.26 (236.5)	9.13 (210.5)

^a 6aa is not a minimum at the BHLYP level.

TABLE 16: Comparison of the Adiabatic Electron Affinities EA_{ad} (in eV) for Br₂F_n, with BrCIF_n, and BrF_n (*n* = 0–6) with the DZP++BHLYP Method^a

<i>n</i>	Br ₂ F _n	BrCIF _n ^b	BrF _{n+1} ^c
0	3.01	3.05	2.64
1	4.74	4.88	4.78
2	4.35	4.35	3.77
3	5.85	5.26	5.58
4	4.49	5.25	4.24
5	5.94		5.59
6	4.20		

^a Without ZPVE corrections. ^b Reference 6. ^c Reference 5.

mental EA is available, are also studied (Table 15). Although all of the DFT predicted EA_{ad} for Br₂ are higher than the experimental value (2.60 eV),²⁸ apart from B3P86, the other DFT methods do a fair job with deviations of 0.35 (BLYP), 0.41 (BHLYP), 0.46 (BP86), and 0.51 eV (B3LYP). Since the BHLYP method appeared to be the best in the predictions of electron affinities of bromine and chlorine fluorides,^{5,25} we may list the EA_{ad} values predicted by BHLYP here, which are 4.74 eV for Br₂F, 4.35 eV for Br₂F₂, 5.85 eV for Br₂F₃, 4.49 eV for Br₂F₄, 5.94 eV for Br₂F₅, and 4.20 eV for Br₂F₆. All of the predicted EAs are large, suggesting that the anions Br₂F_n[−] should be observable. For Br₂F_n with even number *n* (closed-shell), the EA_{ad} values are less large, whereas for Br₂F_n with odd number *n* (open-shell), the EA_{ad} values are larger, since they add the last electron to form closed-shell systems. The EA_{ad} values are in the range of 4.0–6.0 eV and close to those of other interhalogen compounds, such as BrCIF_n and BrF_n.^{5,6} The comparison of these three series is shown in Table 16. The ZPVE corrections to the EA_{ad} values are quite small, with most of these being less than 0.04 eV.

Dissociation Energies for Br₂F_n/Br₂F_n[−]. The first bond dissociation energies for neutral Br₂F_n (*n* = 1–6) and the anions Br₂F_n[−] (*n* = 1–6) are computed as the differences of the total energies in the following ways. The first dissociation energies for the neutrals Br₂F_n (*n* = 1–6) refers to the reactions



The first dissociation energies for the anions in contrast refer

to two different reactions

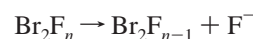
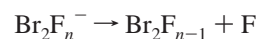


Table 17 lists the neutral Br₂F_n dissociation energies. It is seen that the ground states of all the Br₂F_n and Br₂F_n[−] species are thermodynamically stable. To our knowledge, there are no experimental dissociation energies for the Br₂F_n systems for comparison. As in previous studies,^{5,6,16,25} the BHLYP predictions for the dissociation energies are quite different from those predicted by the other four methods, and they are the least reliable. This is because the BHLYP method incorporates the Hartree–Fock (HF) approximation to the greatest degree, and the HF method is known to perform poorly for bond-breaking processes. Except for BHLYP, the dissociation energies predicted by the other DFT methods are in reasonable agreement with each other, although the pure DFT methods (BP86 and BLYP) yield somewhat larger *D_e* values than those obtained using the hybrid methods (B3P86 and B3LYP). We suspect that the B3LYP thermochemistry predictions are the most reliable. The dissociation energies for Br₂F_n with even *n* are larger than those with odd *n*. This zigzag feature may be readily explained. When *n* is an even number, the Br₂F_n systems are the more stable closed-shell systems, and the Br₂F_{n−1} systems are open-shell systems, so the dissociation energies for Br₂F_n → Br₂F_{n−1} + F are relatively larger. When *n* is odd, the situation is opposite, so the dissociation energies are relatively smaller.

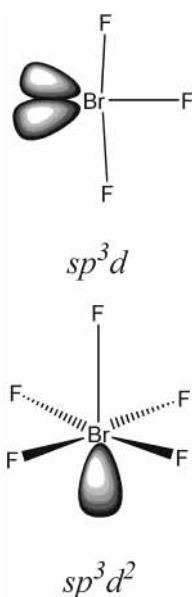
Table 18 lists the corresponding anion dissociation energies. Again, the BHLYP results are different from those obtained with other methods. The zigzag phenomenon can also be observed for the reaction Br₂F_n[−] → Br₂F_{n−1}[−] + F, but the dissociation energies for Br₂F_n with even *n* are smaller than those with odd *n*. The zigzag phenomenon is not noticeable for the anion reactions Br₂F_n[−] → Br₂F_{n−1} + F, because Br₂F_n[−] and Br₂F_{n−1} are either closed shell or open-shell. There are no experimental dissociation energies available for comparison, and we hope our theoretical predictions may stimulate new experimental studies.

TABLE 17: Dissociation Energies (in eV, or in kcal/mol in parentheses) for the Neutral Br_2F_n ($n = 1-6$) Systems^a

	BHLYP	B3P86	B3LYP	BP86	BLYP
Br_2F (1na) \rightarrow Br_2 ($^1\Sigma_g^+$) + F	0.39 (9.0)	1.19 (27.5)	1.14 (26.2)	1.75 (40.3)	1.72 (39.7)
Br_2F_2 (2na) \rightarrow Br_2F (1na) + F	1.51 (34.9)	2.15 (49.5)	2.00 (46.0)	2.33 (53.7)	2.21 (51.0)
Br_2F_3 (3na) \rightarrow Br_2F_2 (2na) + F	1.00 (23.0)	1.73 (40.0)	1.72 (39.6)	2.20 (50.7)	2.20 (50.7)
Br_2F_4 (4na) \rightarrow Br_2F_3 (3na) + F	1.78 (41.0)	2.06 (47.4)	1.92 (44.3)	2.22 (51.1)	2.07 (47.8)
Br_2F_5 (5na) \rightarrow Br_2F_4 (4na) + F	0.71 (16.4)	1.47 (34.0)	1.43 (32.9)	2.02 (46.7)	2.02 (46.6)
Br_2F_6 (6na) \rightarrow Br_2F_5 (5na) + F	1.79 (41.3)	2.42 (55.9)	2.25 (51.9)	2.54 (58.6)	2.40 (55.3)

^a Not corrected with ZPVE.**TABLE 18: Dissociation Energies (in eV, or in kcal/mol in Parentheses) for the Anionic Br_2F_n^- ($n = 1-6$) Systems^a**

	BHLYP	B3P86	B3LYP	BP86	BLYP
Br_2F^- (1aa) \rightarrow Br_2^- ($^2\Sigma_u^+$) + F	2.12 (48.9)	2.87 (66.2)	2.74 (63.2)	3.21 (74.0)	3.11 (71.6)
Br_2F_2^- (2aa) \rightarrow Br_2F^- (1aa) + F	1.12 (25.9)	1.67 (38.6)	1.65 (38.1)	2.00 (46.2)	2.02 (46.5)
Br_2F_3^- (3aa) \rightarrow Br_2F_2^- (2aa) + F	2.50 (57.7)	2.96 (68.3)	2.89 (66.6)	3.13 (72.1)	3.08 (71.0)
Br_2F_4^- (4aa) \rightarrow Br_2F_3^- (3aa) + F	0.41 (9.5)	1.42 (32.7)	1.32 (30.4)	2.01 (46.3)	1.95 (45.0)
Br_2F_5^- (5aa) \rightarrow Br_2F_4^- (4aa) + F	2.16 (49.8)	2.61 (60.3)	2.50 (57.7)	2.75 (63.3)	2.64 (60.8)
Br_2F_6^- (6aa) \rightarrow Br_2F_5^- (5aa) + F	0.06 (1.3)	1.13 (26.1)	1.03 (23.8)	1.82 (42.0)	1.76 (40.5)
Br_2F^- (1aa) \rightarrow Br_2 ($1\Sigma_g^-$) + F ⁻	2.19 (50.5)	2.41 (55.6)	2.30 (53.1)	2.50 (57.6)	2.38 (55.0)
Br_2F_2^- (2aa) \rightarrow Br_2F (1na) + F ⁻	2.92 (67.4)	2.89 (66.8)	2.82 (65.0)	2.76 (63.6)	2.68 (61.8)
Br_2F_3^- (3aa) \rightarrow Br_2F_2 (2na) + F ⁻	3.91 (90.2)	3.71 (85.5)	3.71 (85.5)	3.56 (82.0)	3.55 (81.8)
Br_2F_4^- (4aa) \rightarrow Br_2F_3 (3na) + F	3.32 (76.7)	3.39 (78.2)	3.31 (76.3)	3.36 (77.6)	3.30 (76.1)
Br_2F_5^- (5aa) \rightarrow Br_2F_4 (4na) + F ⁻	3.71 (85.5)	3.95 (91.1)	3.89 (89.7)	3.89 (89.8)	3.87 (89.2)
Br_2F_6^- (6aa) \rightarrow Br_2F_5 (5na) + F ⁻	3.05 (70.4)	3.61 (83.2)	3.50 (80.6)	3.69 (85.1)	3.60 (83.1)

^a Not corrected with ZPVE. 9**Figure 13.** Structures with sp^3d and sp^3d^2 model hybridization. The former case (BrF_3) displays a trigonal bipyramidal electronic geometry and a T-shaped molecular structure. The latter case (BrF_5) displays an octahedral electronic geometry and a square pyramidal molecular structure. These simple (indeed naive) ideas help explain the less conventional structure predicted in this research.

Conclusions

In the present paper, we have optimized more than 60 stationary point structures for the $\text{Br}_2\text{F}_n/\text{Br}_2\text{F}_n^-$ systems with five selected DFT methods. Most of these have not been previously reported, and many have unusual molecular structures. Many additional structures (not reported here) have been explored and found either (a) not to be stationary points or (b) to be very high lying energetically. For the open shell systems in the present study, the spin contamination is very small. For example, the estimated $\langle S^2 \rangle$ value (forcing the DFT orbitals into a single determinant) for the doublet states is less than 0.76, with a few exceptions. The worst cases are structure 2ae with the BHLYP method (0.82) and structure 2af with BHLYP (0.81).

The optimized geometries for the $\text{Br}_2\text{F}_n/\text{Br}_2\text{F}_n^-$ systems reveal many T-shaped and rectangular-pyramidal structures. That is, the bond angles for these interhalogen compounds show some inclination to be 90° or 180° . This may be rationalized in terms of the sp^3d hybridization (T-shaped) or the sp^3d^2 hybridization (rectangular pyramidal) models for the central Br atomic orbitals (Figure 13).

Compared with experimental EA values for Br_2 ,^{28,29} our selected DFT methods seem to give reasonable predictions for electron affinities. Table 15 shows that our final theoretical predictions (BHLYP method) of the adiabatic electron affinities (EA_{ad}) are 4.74 (Br_2F), 4.35 (Br_2F_2), 5.85 (Br_2F_3), 4.49 (Br_2F_4), 5.94 (Br_2F_5), and 4.20 eV (Br_2F_6). These large electron affinities suggest that the Br_2F_n^- species should be observable in the laboratory. The molecular structures of these systems appear best predicted by the BHLYP method (although structures 2nb, 3nb, and 3nc appear to be an exception), whereas the thermochemistry is best treated with B3LYP.

The present research may be viewed as exploratory theoretical chemistry. Our goal is to provide a broad and qualitative view of the landscapes of the different potential energy surfaces. Many controversies remain. These will only be resolved by definitive new experiments or by further theoretical methods using convergent quantum mechanical methods such as advanced coupled cluster theory with large basis sets.

Acknowledgment. This research was supported by Key Laboratory of Theoretical and Computational Chemistry of Jilin University of China and the U.S National Science Foundation, Grant No. CHE-0136186.

References and Notes

- (1) Barker, J. R. *Progress and Problems in Atmospheric Chemistry*; World Scientific: Singapore, 1995.
- (2) Hebestreit, K.; Stutz, J.; Rosen, D.; Matveiv, D.; Peleg, M.; Luria, M.; Platt, U. *Science* **1999**, 283, 55.
- (3) Larichev, M.; Maguin, F.; Le Bras, G.; Poulet, G. *J. Phys. Chem.* **1995**, 99, 15911.
- (4) Vogt, R.; Crutzen, P. J.; Sander, R. *Nature* **1996**, 383, 327.
- (5) Pak, C.; Xie, Y.; Van Huis, T. J.; Schaefer, H. F. *J. Am. Chem. Soc.* **1998**, 120, 11115.
- (6) Ignatyev, I. S.; Schaefer, H. F. *J. Am. Chem. Soc.* **1999**, 121, 6904.

- (7) The BHandHLYP method implemented in the Gaussian programs has the formula, $0.5*\text{Ex(LSDA)}+0.5*\text{Ex(HF)}+0.5*\text{Delta-Ex(B88)}+\text{Ec(LYP)}$, which is *not* precisely the formulation proposed by A. D. Becke in his paper, *J. Chem. Phys.* **1993**, *98*, 1372.
- (8) Lee, C.; Yang, W.; Parr, R. G. *Phys. Rev. B* **1988**, *37*, 785.
- (9) Becke, A. D. *J. Chem. Phys.* **1993**, *98*, 5648.
- (10) Perdew, J. P. *Phys. Rev. B* **1986**, *33*, 8822; *34*, 7406.
- (11) Becke, A. D. *Phys. Rev. A* **1988**, *37*, 785.
- (12) Schäfer, A.; Horn, H.; Ahlrichs, R. *J. Chem. Phys.* **1992**, *97*, 2571.
- (13) Huzinaga, S. *J. Chem. Phys.* **1965**, *42*, 1293. Duning, T. H. *J. Chem. Phys.* **1970**, *53*, 2823.
- (14) Frisch, M. J.; Trucks, G. W.; Schlegel, H. B.; Scuseria, G. E.; Robb, M. A.; Cheeseman, J. R.; Zakrzewski, V. G.; Montgomery, J. A., Jr.; Stratmann, R. E.; Burant, J. C.; Dapprich, S.; Millam, J. M.; Daniels, A. D.; Kudin, K. N.; Strain, M. C.; Farkas, O.; Tomasi, J.; Barone, V.; Cossi, M.; Cammi, R.; Mennucci, B.; Pomelli, C.; Adamo, C.; Clifford, S.; Ochterski, J.; Petersson, G. A.; Ayala, P. Y.; Cui, Q.; Morokuma, K.; Malick, D. K.; Rabuck, A. D.; Raghavachari, K.; Foresman, J. B.; Cioslowski, J.; Ortiz, J. V.; Stefanov, B. B.; Liu, G.; Liashenko, A.; Piskorz, P.; Komaromi, I.; Gomperts, R.; Martin, R. L.; Fox, D. J.; Keith, T.; Al-Laham, M. A.; Peng, C. Y.; Nanayakkara, A.; Gonzalez, C.; Challacombe, M.; Gill, P. M. W.; Johnson, B. G.; Chen, W.; Wong, M. W.; Andres, J. L.; Head-Gordon, M.; Replogle, E. S.; Pople, J. A. *Gaussian 98*, revision A.6; Gaussian, Inc.: Pittsburgh, PA, 1998.
- (15) (a) Huber, K. P.; Herzberg, G. *Molecular Spectra and Molecular Structure. IV. Constants of Diatomic Molecules*; Van Nostrand: New York, 1979. (b) Fosca, C.; Li, H.; Bernath, P. F. *J. Mol. Spectrosc.* **2000**, *200*, 104.
- (16) Pak, C.; Xie, Y.; Schaefer, H. F. *Mol. Phys.* **2003**, *101*, 211.
- (17) Ayala, J. A.; Wentworth, W. E.; Chen, E. C. M. *J. Phys. Chem.* **1981**, *85*, 768.
- (18) Wright, C. A.; Ault, B. S.; Andrews, L. *Inorg. Chem.* **1976**, *15*, 2147.
- (19) Willis, R. E.; Clark, W. W. *J. Chem. Phys.* **1980**, *72*, 4946.
- (20) Magnuson, D. W. *J. Chem. Phys.* **1957**, *27*, 223.
- (21) Robliette, A. G.; Bradley, R. H.; Brier, P. N. *Chem. Commun.* **1971**, *23*, 1567.
- (22) Edward, A. J.; Jones, G. R. *J. Chem. Soc. A* **1969**, 1936.
- (23) Gaydon, A. G. *Dissociation Energies and Spectra of Diatomic Molecules*; Chapman and Hall; London, 1968.
- (24) Boese, D.; Martin, J. M. L.; Handy, N. C. *J. Chem. Phys.* **2003**, *119*, 3005.
- (25) Van Huis, T. J.; Galbraith, J. M.; Schaefer, H. F. *Mol. Phys.* **1996**, *89*, 607.
- (26) Prochaska, E. S.; Andrews, L.; Smyrl, N. R.; Mamantov, G. *Inorg. Chem.* **1978**, *17*, 970.
- (27) Rienstra-Kiracofe, J. C.; Tschumper, G. S.; Schaefer, H. F.; Nandi, S.; Ellison, G. B. *Chem. Rev.* **2002**, *102*, 231.
- (28) Dispert, H.; Lacmann, K. *Chem. Phys. Lett.* **1977**, *47*, 533.
- (29) Drzaic, P. S.; Marks, J.; Brauman, J. I. in *Gas-Phase Ion Chemistry*; Bowers, M. T., Ed.; Academic Press: New York, 1984; Vol. 3, p 167.